4

Spatially Sampled Robust Repetitive Control

Cheng-Lun Chen[1] and George T.-C. Chiu[2]
[1]*National Chung Hsing University;*
[2]*Purdue University, West Lafayette;*
[1]*Taiwan, R.O.C.*
[2]*USA*

1. Introduction

Repetitive control is one control algorithm based on the Internal Model Principle (Francis & Wonham, 1976) and has been widely implemented in various applications. A repetitive control based system has been shown to work well for tracking periodic reference commands or for rejecting periodic disturbances. Although the idea has been verified as early as 1981 (Inoue et al., 1981), a rigorous analysis and synthesis of repetitive controllers for continuous-time systems was not proposed until 1989, by Hara et al. (Hara et al., 1988). Tomizuka et al. (Tomizuka et al., 1989) addressed the analysis and synthesis of discrete-time repetitive controller, considering the fact that digital implementation of a repetitive controller is simpler and more straightforward. Since then, repetitive control has gained popularity in applications where periodic disturbances rejection or repetitive tracking are required, see (Wang et al., 2009; Cuiyan et al., 2004) and the references therein. These include controls of disk drive servo (Tomizuka et al., 1989; Guo, 1997; Moon et al., 1998), hydraulic closed-loop servo for material testing (Srinivasan & Shaw, 1993), vibration suppression (Hillerstrom, 1996), rejection of load disturbances in steel casting process (Manayathara et al., 1996), servo control for a positioning table (Yamada et al., 1999), X-Y table (Tung et al., 1993), noncircular turning process (Alter & Tsao, 1994), motor speed ripple reduction (Godler et al., 1995; Rodriguez et al., 2000), and eccentricity compensation (Garimella & Srinivasan, 1996).

In literatures, repetitive controllers are synthesized and operate in time domain, which is in accordance with the fact that models or differential equations of physical systems are mostly derived using time as the independent variable. One of the key steps for designing a repetitive controller is to determine the period, or equivalently, the number of delay taps (q^{-1}, q is the one step advance operator). This can usually be done by analyzing the periodic tracking or disturbance signal using techniques such as fast Fourier transform (FFT). To ensure effectiveness of the design, an underlying assumption is that the frequency constitutions of the periodic tracking or disturbance signal do not vary with respect to time, which corresponds to a stationary or time-invariant frequency spectrum of the signal. This assumption can be satisfied when the design objective is to track a pre-specified periodic trajectory. However, it might be violated for disturbance rejection problems where the frequency constitutions of the disturbance are time-varying. For a motion system with rotary components such as gear-train, the disturbances due to gear

eccentricity or tooth profile error are inherently angular displacement dependent or spatially periodic. They are periodic with respect to angular displacement, but not necessarily periodic with respect to time. Gear eccentricity induces disturbances with period equal to one revolution and tooth profile error induces disturbances with fundamental frequency equal to the number of teeth per revolution. The spatial periods for these two types of disturbances do not change with the angular velocity. However, the corresponding temporal frequencies will be proportional to the angular velocity and vary accordingly when the system operates at variable speeds. As an example, for a single stage motor/gear transmission system operating an output speed of v revolution per second, the eccentricity error of the final gear will show up as a periodic disturbance with temporal frequency of v Hz. As the operating speed changes, a proportional changes to the temporal frequency of the disturbance will occur whereas its spatial frequency is fixed at 1 cycle per revolution. Suppose that a repetitive controller is implemented using a constant-angular-displacement sampling period (spatially sampled) approach, e.g., m samples per revolution of the final gear, to tackle this disturbance. The number of required delay taps, which reflects the period of the disturbance, will be a constant m regardless of the angular velocity. On the other hand, a repetitive controller synthesized using the conventional approach, i.e., based on the temporal frequency of the disturbance (v Hz), and implemented with constant-time sampling period will not be effective if the number of delay taps for the repetitive controller is not tuned/adapted in real-time in accordance with the angular velocity. If the period fluctuation is small, methods have been shown to improve the robustness of the repetitive controller by increasing the notch width in the frequency domain of the repetitive controller at the cost of reduced attenuation for the periodic disturbance (Onuki & Ishioka, 2001). When the period variation is large, there are two approaches to address the varying period in a repetitive control framework. For situation where the period variation can not be measured or unknown, adaptive control approaches have been shown to be effective in adapting the period of the repetitive controller (Hillerstrom, 1996; Manayathara et al., 1996; Wit & Praly, 2000) at the expense of response time and transient response. When the period variation is known or can be measured, such as the case in gear noise induced disturbance, better trade-off between period adaptability and effectiveness of repetitive control can be made.

Recent researches started studying control problems of rejecting/tracking spatially periodic disturbances/references in spatial domain, i.e., using spatially sampled repetitive controllers. As explained earlier, a spatially sampled repetitive controller has its repetitive kernel (i.e., e^{-st} or z^{-N} with positive feedback) synthesized and operate with respect to angular displacement. Hence its capability for rejecting/tracking spatially periodic disturbances/references will not degrade when the controlled system operates at varying speed. Note that a typical repetitive control system consists of repetitive (i.e., a repetitive kernel) and non-repetitive (e.g., a stabilizing controller) portions. Given a time-domain open-loop system and with the repetitive kernel to be synthesized and implemented in spatial domain, design of the non-repetitive portion that properly interfaces the repetitive kernel and the open-loop system actually poses a challenge. (Nakano et al., 1996) initiated a fundamental design of spatially sampled repetitive controller in 1996. Although the proposed design is rudimentary due to its focus on simple linear time-invariant systems, it has recently motivated several more advanced designs (Mahawan & Luo, 2000; Chen et al., 2006). The design started by transforming a given open-loop system in time domain into one

in spatial domain. Specifically, the variable of time is rendered implicit for the transformed system in spatial domain with angular displacement being the new independent variable. This is attained by using the relationship between angular displacement and velocity along with imposing an assumption of bijective mapping between time and angular displacement. The resulting nonlinear system was linearized at a fixed angular velocity and a stabilizing controller with built-in repetitive control action was synthesized. In (Chen et al., 2006), robust control methods were employed to address issues associated with using a linearized plant model in the controller synthesis and actuator saturation. Although effective for small angular velocity fluctuations, the effectiveness of a linearized approach is limited when the application requires a large variation in operating speed. (Mahawan & Luo, 2000) demonstrated the feasibility of augmenting a spatially sampled repetitive controller to a time-sampled stabilizing controller, where no reformulation and linearization of the open-loop plant model is required. However, the complexity of the method lies in the need to solve an optimization problem in real-time to synchronize the hardware and software interrupts associated with time and spatial sampling, respectively. In addition, although reasonable for trajectory tracking, the assumption of a known mapping between time and angular displacement is rarely applicable for disturbance rejection applications. The lack of considerations to modeling uncertainty is another area that can be improved from the methods proposed in (Nakano et al., 1996) and (Mahawan & Luo, 2000). Instead of linearizing the resulting nonlinear plant model, (Chen and Chiu, 2008) shows that the nonlinear plant model can be formulated into a quasi-linear parameter varying (quasi-LPV) system, where the angular speed is one of the measurable varying parameters. Leveraging existing results in controller synthesis for LPV systems (Becker & Packard, 1994; Apkarian et al., 1995; Gahinet, 1996; Gahinet & Apkarian, 1994, 1995) and the robust repetitive design formulation outlined in (Chen et al., 2006; Hanson & Tsao, 2000), an LPV gain-scheduling controller can be obtained that addresses bounded modeling uncertainties, actuator saturation and spatially periodic disturbances.

This book chapter will provide the reader with a review and summary of recent advances in design of spatially sampled repetitive control systems. Specifically, we will elaborate on a few designs which account for the robustness property of the system, i.e., capability in tackling modeling uncertainties and actuator saturation. Current issues and future research directions will also be discussed. The outline of this chapter is as follows:

Section 2 demonstrates how to transform a generic time-domain system into its counterpart in spatial domain. It is also shown that nonlinearity such as actuator saturation may be properly modeled and incorporated into the spatial-domain open-loop system.

Section 3 presents a design of spatially sampled robust repetitive control. A well-known approach for designing controllers for nonlinear systems with a well defined operating point is to first linearize the system around the nominal operating point. Once the linear system is extracted, linear robust design paradigm can be applied to establish a design framework with embedded repetitive controller.

Section 4 presents another design of spatially sampled robust repetitive control. By reformulating the transformed spatial-domain system as a quasi-linear parameter varying (quasi-LPV) system, we gain access to the LPV design framework for gain-scheduling controllers. Hence, an LPV gain-scheduling repetitive control (LPVRC) system can be synthesized by augmenting the repetitive controller with the LPV controller. The LPVRC design is superior to others in the sense that 1) It requires less computation effort when compared to nonlinear design; 2) It is robust to spatially periodic disturbances when

compared to temporal-based design; 3) It allows wider operation range when compared to designs using linearization approaches.
Section 5 concludes the chapter and points out issues and future research directions relevant to spatially sampled robust repetitive control.

2. Problem formulation – Position-invariant rotary systems

In this section, we show how a generic nonlinear time-invariant (NTI) model can be transformed into a nonlinear position-invariant (NPI; as opposed to the definition of time-invariant) model by choosing an alternate independent variable (angular displacement instead of time) and defining a new set of states (or coordinates) with respect to the angular displacement. Note that the transformation described here is equivalent to a nonlinear coordinate transformation or a diffeomorphism. The NPI model will be used for the subsequent design and discussion. In Section 2.1, we further demonstrate this transformation for a typical linear time-invariant (LTI) rotary system with actuator saturation, which will be utilized in subsequent design.
Consider the mathematical model of a single-input single-output (SISO) nth-order NTI system with model uncertainties, and subject to output disturbance, i.e.,

$$\begin{aligned} \dot{x}(t) &= \left[f_t\left(x(t), f_f\right) + \Delta f_t\left(x(t), f_f\right)\right] + \left[g_t\left(x(t), f_g\right) + \Delta g_t\left(x(t), f_g\right)\right] u(t) \\ y &= \Psi x(t) + d(t) = x_n(t) + d_y(t) \end{aligned} \tag{1}$$

where $x(t) = \left[x_1(t) \quad \cdots \quad x_n(t)\right]^T$, $\Psi = \left[0 \quad \cdots \quad 0 \quad 1\right]$, $u(t)$ and $y(t)$ correspond to control input and measured output angular velocity of the system, respectively. $d_y(t)$ represents a class of position-dependent disturbances which constitutes bounded spatially periodic and non-periodic components. Here we refer non-periodic disturbances to signals whose Fourier transform or power spectral density is zero above a certain finite frequency. The only available information of the disturbances is the number of distinctive spatial frequencies and the spectrum distribution for non-periodic disturbance components. $f_t\left(x(t), \phi_f\right)$ and $g_t\left(x(t), \phi_g\right)$ are known vector-valued functions with unknown but bounded system parameters, i.e., $\phi_f = \left[\phi_{f1} \quad \cdots \quad \phi_{fk}\right]$ and $\phi_g = \left[\phi_{g1} \quad \cdots \quad \phi_{gl}\right]$; $\Delta f_t\left(x(t), \phi_f\right)$ and $\Delta g_t\left(x(t), \phi_g\right)$ represent unstructured modeling inaccuracy, which are also assumed to be bounded. Instead of using time t as the independent variable, consider an alternate independent variable $\theta = \lambda(t)$, i.e., the angular displacement. Since by definition

$$\lambda(t) = \int_0^t \omega(\tau) d\tau + \lambda(0),$$

where $\omega(t)$ is the angular velocity, the following condition

$$\omega(t) = \frac{d\theta}{dt} > 0, \ \forall \ t > 0 \tag{2}$$

will guarantee that $\lambda(t)$ is strictly monotonic such that $t = \lambda^{-1}(\theta)$ exists. Thus all the variables in the time domain can be transformed into their counterparts in the θ-domain, i.e.,

$$\hat{x}(\theta) = x(\lambda^{-1}(\theta)),\ \hat{y}(\theta) = y(\lambda^{-1}(\theta)),$$
$$\hat{u}(\theta) = u(\lambda^{-1}(\theta)),\ \hat{d}(\theta) = d(\lambda^{-1}(\theta)),$$
$$\hat{\omega}(\theta) = \omega(\lambda^{-1}(\theta)),$$

where we denote $\hat{\bullet}$ as the θ-domain representation of $\bullet$. Note that, in practice, (2) can usually be satisfied for most rotary motion system where the rotary component rotates only in one direction. Since

$$\frac{dx(t)}{dt} = \frac{d\theta}{dt}\frac{d\hat{x}(\theta)}{d\theta} = \hat{\omega}(\theta)\frac{d\hat{x}(\theta)}{d\theta}$$

(1) may be rewritten as

$$\begin{aligned} \hat{\omega}(\theta)\frac{d\hat{x}(\theta)}{d\theta} &= \left[f_t\left(\hat{x}(\theta), \phi_f\right) + \Delta f_t\left(\hat{x}(\theta), \phi_f\right)\right] + \left[g_t\left(\hat{x}(\theta), \phi_g\right) + \Delta g_t\left(\hat{x}(\theta), \phi_g\right)\right]\hat{u}(\theta) \\ \hat{y}(\theta) &= \Psi\hat{x}(\theta) + \hat{d}_y(\theta) = \hat{x}_n(\theta) + \hat{d}_y(\theta). \end{aligned} \tag{3}$$

Equation (3) can be regarded as an NPI system with the angular displacement θ as the independent variable. Note that the concept of transfer function is still valid for linear position-invariant systems if we define the Laplace transform of a signal $\hat{g}(\theta)$ in the angular displacement domain as

$$\hat{G}(\tilde{s}) = \int_0^\infty \hat{g}(\theta)e^{-\tilde{s}\theta}d\theta\ .$$

This definition will be useful for describing the linear portion of the overall control system.

2.1 Transformation of an LTI rotary system with actuator saturation

Suppose a state space realization of an LTI model for a typical rotary system can be expressed as

$$\begin{bmatrix} \dot{x}(t) \\ z(t) \\ y(t) \end{bmatrix} = \begin{bmatrix} A & B_v & B_u \\ C_z & D_{zv} & D_{zu} \\ C_y & D_{yv} & 0 \end{bmatrix} \begin{bmatrix} x(t) \\ v(t) \\ u(t) \end{bmatrix} \tag{4}$$

where $x(t)$ is the system state vector, $\dot{x}(t)$ denotes the time derivative of the state vector, $v(t)$ is the output disturbance vector that contains spatially periodic components, $z(t)$ denotes the output vector related to system performance, $y(t)$ is the measurement vector, and $u(t)$ is the control input vector. Those signals are linearly related by the matrices shown in (4), i.e., A, B_v, C_z, etc. and all of the matrices and vectors are assumed to have compatible dimensions. If $\Phi(t)$ is a strictly monotonic function of t such that its inverse $t = \Phi^{-1}(t)$ exists and does not vanish, variables in time domain will have a well defined counterpart in the θ-domain, i.e.,

$$\tilde{x}(\theta) \triangleq x(\Phi^{-1}(\theta)),\ \tilde{z}(\theta) \triangleq z(\Phi^{-1}(\theta)),$$
$$\tilde{y}(\theta) \triangleq y(\Phi^{-1}(\theta)),\ \tilde{v}(\theta) \triangleq v(\Phi^{-1}(\theta)),\ \text{and}\ \tilde{u}(\theta) \triangleq u(\Phi^{-1}(\theta)).$$

Suppose the angular velocity can be measured in real-time and written as

$$\tilde{\omega}(\theta) = C_{\omega}\tilde{x}(\theta) + \omega_0 \neq 0, \tag{5}$$

where ω_0 is the nominal angular velocity and C_{ω} is an appropriate output matrix. Applying the aforementioned transformation, substituting (5) into (4), and imposing the saturation function

$$sat(u) = \begin{cases} u_{\max}, & u \geq u_{\max} \\ u, & u_{\min} < u < u_{\max} \\ u_{\min}, & u \leq u_{\min} \end{cases}$$

on $\tilde{u}(\theta)$, we have

$$\begin{bmatrix} \dot{\tilde{x}}(\theta) \\ \tilde{z}(\theta) \\ \tilde{y}(\theta) \end{bmatrix} = \begin{bmatrix} A/(C_{\omega}\tilde{x} + \omega_0) & B_v/(C_{\omega}\tilde{x} + \omega_0) & B_u/(C_{\omega}\tilde{x} + \omega_0) \\ C_z & D_{zv} & D_{zu} \\ C_y & D_{yv} & 0 \end{bmatrix} \begin{bmatrix} \tilde{x}(\theta) \\ \tilde{v}(\theta) \\ sat(\tilde{u}(\theta)) \end{bmatrix}. \tag{6}$$

The system expressed by (6) is an angular displacement reformulated (ADR) system with the angular displacement θ as the independent variable.

3. Linear spatially sampled robust repetitive control

Linear robust controller design is aiming at synthesizing a feedback controller so that stability and performance of the overall (closed-loop) control system is insensitive (i.e., robust) to external disturbances and model uncertainties. There are four popular terms used to characterize the performance of a linear feedback control system, namely nominal stability, nominal performance, robust stability, and robust performance (Zhou & Doyle, 1997). We say that a feedback control system is stable if its output signals are bounded when subject to bounded input signals. A feedback control system meets (steady-state) performance if it is stable and the ratio of the sizes (measured by a mathematical norm, e.g., 2-norm) of its output to input signals is bounded above by certain frequency dependent number. In most cases, stability comes first, and performance comes next in the priority of the design. Nominal stability/performance is to be satisfied by controller design only for a plant, i.e., the model of the to-be-controlled system (free of parameter uncertainty), while robust stability/performance is to be satisfied by more challenged design for a set of plants, which include the nominal one and those due to plant parameter variation. Linear fractional transformation (LFT) is a popular and effective technique to formulate and pose a robust control design problem as will be demonstrated next.

3.1 Synthesis of the robust controller

Start the design by first looking at the LFT representation of the desired closed loop control system depicted in Fig. 1, which incorporate two motors as the actuators. An LFT representation basically consists of three blocks: generalized plant, generalized uncertainty, and the stabilizing controller. Several variables and components need to be explained here. First, the generalized plant $P(z)$ (i.e., discrete-position system with z denoted the variable

used in the z-transform) includes the plant, and all linear weighting filters whose magnitude responses are used to specify the frequency-wise bounds on the output signals and modeling uncertainty. All mathematical operations within the generalized plant are either addition of two signals or scalar multiplication of signals, which renders $P(z)$ linear. Note that only motor actuators are considered in the framework and driven by the control input u calculated by the controller $K(z)$. Other type of actuators can also be considered. Second, the inputs to the controller y are output signal measurement, e.g. velocity error from the rotary component. Third, the variable w includes those external signals such as periodic disturbances while the variable z includes those physical quantities which are important to system performance. Furthermore, p and q represent the input and output of the generalized uncertainty which is formed by all the uncertainty blocks from the generalized plant. The uncertainty blocks are usually formed by the modeling error and plant nonlinearity. There exist standard procedures and techniques to 'pull out' uncertainties from the generalized plant (Zhou & Doyle, 1997).

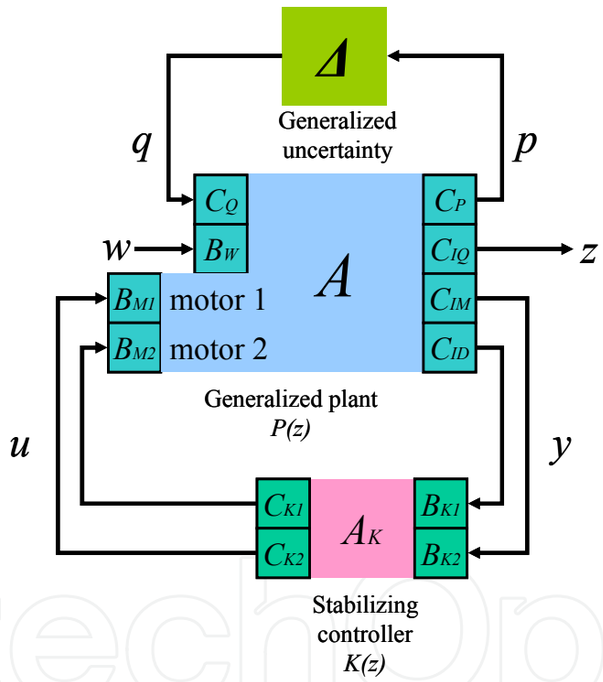

Fig. 1. LFT representation of the EP closed-loop control system using motor actuators.

Based on the LFT representation, a discrete-position state space realization of the to-be-controlled system (the generalized plant plus the generalized uncertainty) can be written as

$$\begin{aligned} x_{k+1} &= Ax_k + [B_{M1} \quad B_{M2}]u_k + B_W w_k, \\ y_k &= \begin{bmatrix} C_{IM} \\ C_{ID} \end{bmatrix} x_k + D_{YW} w_k, \\ z_k &= C_{IQ} x_k + D_{ZW} w_k, \\ q &= \Delta p, \end{aligned} \tag{7}$$

and the optimal stabilizing controller $K(z)$, parameters of which stabilize the system and also minimize the size of the transfer function from w to z (or the ratio between the sizes of w and z if induced matrix norm is used) in the presence of the generalized uncertainty, can be represented as

$$K(z) = \begin{bmatrix} C_{K1} \\ C_{K2} \end{bmatrix} (zI - A_K)^{-1} [B_{K1} \quad B_{K2}] + D_K. \tag{8}$$

The corresponding optimization (or robust performance) problem can be formulated as

$$\begin{aligned} &\text{minimize } \left\| H_{wz}(z) \right\| \\ &\text{subject to } K(z) \text{ stabilizes the system,} \end{aligned}$$

where $H_{wz}(z)$ is the transfer function from w to z, and $\|\bullet\|$ is some induced matrix norm. The decision variables to be found are A_K , $[B_{K1} \quad B_{K2}]$, $[C_{K1} \quad C_{K2}]^T$ and D_K . It has been shown that the above problem is nonconvex and a sophisticated search algorithm (e.g., D-K iteration) needs to be implemented in order to locate the global optimal solution. An alternative way is to consider a suboptimal controller which is the solution to the following problem

$$\begin{aligned} &\text{minimize } \left\| H_{qw \to pz}(z) \right\| \\ &\text{subject to } K(z) \text{ stabilizes the system,} \end{aligned}$$

where $H_{qw \to pz}(z)$ is the transfer function from $[q \quad w]$ to $[p \quad z]$, and $\|\bullet\|$ is some induced matrix norm. This is the so-called mixed-sensitivity optimization problem and is convex. There have been standard software tools for solving this type of problems (Gahinet & Nemirovski, 1995).

3.2 Discrete-position model of the system

Suppose that the open-loop LTI system P(s) has a state space realization, i.e.,

$$\begin{aligned} \frac{dx(t)}{dt} &= Ax(t) + B_u u(t) \\ y(t) &= C_y x(t) + D_{yv} v(t), \end{aligned} \tag{9}$$

where $v(t)$ denotes disturbances at the plant output. Equation (9) is basically a simplified version of (4). Instead of using time t as the independent variable, we can pick angular position, $\theta(t)$, as the independent variable, i.e. $\phi = \theta(t)$. Thus in the ϕ -domain Eq. (9) can be expressed as

$$\begin{aligned} \frac{d\phi}{dt}\frac{d\tilde{x}(\phi)}{d\phi} &= A\tilde{x}(\phi) + B_u \tilde{u}(\phi) \\ \tilde{y}(\phi) &= C_y \tilde{x}(\phi) + D_{yv} \tilde{v}(\phi), \end{aligned} \tag{10}$$

where $\tilde{x}(\phi) = x(f^{-1}(\phi))$, $\tilde{u}(\phi) = u(f^{-1}(\phi))$, $\tilde{y}(\phi) = y(f^{-1}(\phi))$, and $\tilde{v}(\phi) = v(f^{-1}(\phi))$.
Linearize the equation around the nominal angular velocity ω_0, we have

$$\begin{aligned} \frac{d\tilde{x}(\theta)}{d\phi} &= \frac{A}{\omega_0}\tilde{x}(\theta) + \frac{B_u}{\omega_0}\tilde{u}(\theta) \\ \tilde{y}(\theta) &= C_y\tilde{x}(\theta) + D_{yv}\tilde{v}(\theta). \end{aligned} \tag{11}$$

Equation (11) is a linear position invariant (LPI) system with the angular position $\theta(t)$ as the independent variable. Note that this transformation will render those position-dependent disturbances within $\tilde{v}$ periodic and stationary. The performance of a repetitive controller synthesized in the θ-domain will not be compromised. Properly choosing spatial sampling frequency T_θ (in number of samples per revolution), we can discretize Eq. (11) and acquire a discrete-position model, i.e.

$$\begin{aligned} \tilde{x}_{k+1} &= e^{\frac{A}{\omega_0}T_\theta}\tilde{x}_k + \left(\int_0^{T_\theta} e^{\frac{A}{\omega_0}\tau} d\tau\right)\frac{B_u}{\omega_0}\tilde{u}_k \\ \tilde{y}_k &= C_y\tilde{x}_k + D_{yv}\tilde{v}_k. \end{aligned} \tag{12}$$

The procedures summarized in the literature (Chen & Chiu, 2001) can now be applied to the plant model expressed in Eq. (12) for synthesizing a two degree of freedom (TDOF) discrete-position robust repetitive controller.

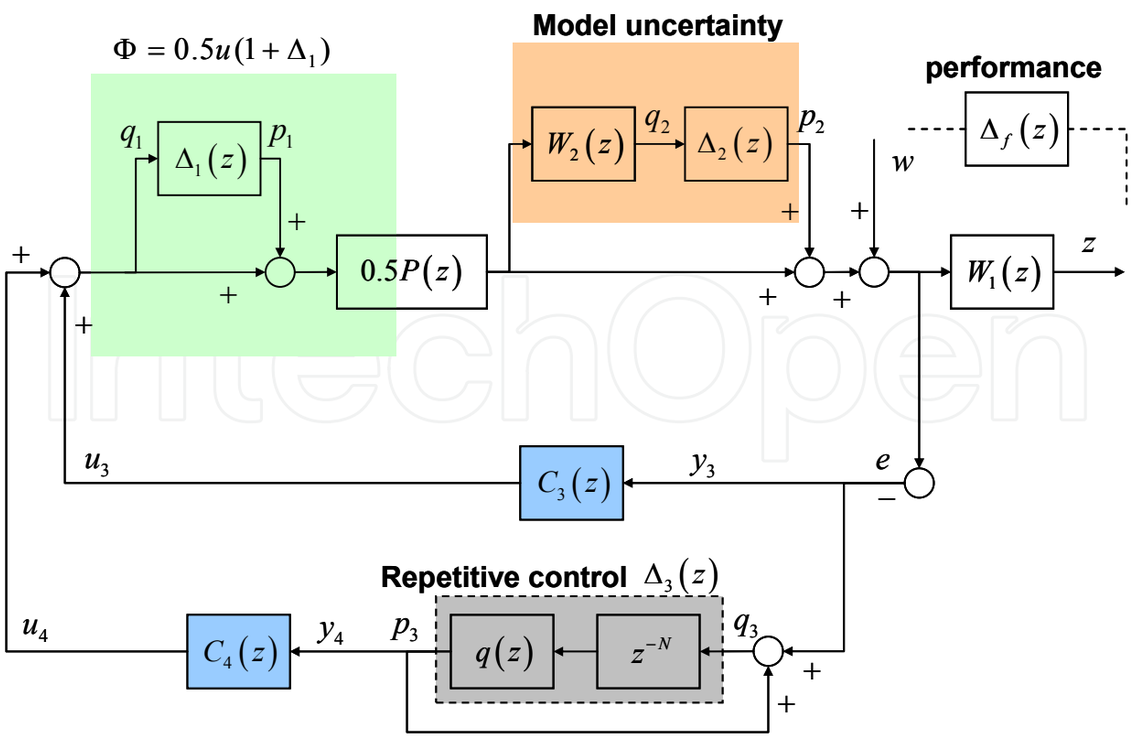

Fig. 2. The proposed TDOF robust repetitive control system.

3.3 TDOF robust repetitive controller

To reduce system sensitivity or increase system robustness to unmodeled dynamics or nonlinearity (i.e. actuator saturation), we can formulate the control problem within a unified linear design framework, i.e. using LFT. The proposed TDOF control structure is depicted in Fig. 2. The actual plant is represented as a saturation element $0.5(1+\Delta_1)$ with $|\Delta_1| \leq 1$ followed by a nominal model $P(z)$ with output multiplicative uncertainties $W_2\Delta_2$. W_2 is the frequency-dependent uncertainty weighting filter such that $\|\Delta_2\|_\infty \leq 1$. It can be picked to be any stable filter with its magnitude upper bounding the multiplicative error between the model and the actual plant, i.e.

$$\left|\frac{\hat{P}\left(e^{jw}\right)-P\left(e^{jw}\right)}{P\left(e^{jw}\right)}\right| \leq \left|W_2\left(e^{jw}\right)\right|, \ \forall w \tag{13}$$

Furthermore, the kernel of the repetitive controller $q(z)z^{-N}$ is replaced by a fictitious uncertainty Δ_3. Also another fictitious uncertainty Δ_f is connected between the disturbance input and plant output. W_1 is the frequency-dependent weighting filter that approximates human contrast sensitivity function (Chen et al., 2003). Thus, a TDOF controller is obtained by solving the following mixed-sensitivity optimization problem given by

$$\gamma_{opt} = \inf_{\text{K stabilizing}} \left\| \begin{matrix} W_1\left(1+PC_4\right)^{-1} \\ C_4P\left(1+C_4P\right)^{-1} \\ -W_2PC_4\left(1+PC_4\right)^{-1} \\ 1-P\left(1-C_4P\right)^{-1}C_3 \end{matrix} \right\|_\infty , \tag{14}$$

where

$$\begin{aligned} P &\triangleq \text{Motor/Gear transmission system} \\ W_1 &\triangleq \text{Performance weighting} \\ W_2 &\triangleq \text{Uncertainty weighting} \\ K &\triangleq \begin{bmatrix} C_3 & C_4 \end{bmatrix} \text{ The TDOF controller} \end{aligned}$$

With upper and lower LFT denoted by $F_u(\cdot,\cdot)$ and $F_l(\cdot,\cdot)$, respectively (Zhou & Doyle, 1997), the robust performance of the designed control system can further be evaluated by looking at the structure singular value of $F_l\left(F_u(M,R),K\right)$ with respect to the uncertainty block $\Delta = diag\left(\Delta_1,\Delta_2,\Delta_f\right)$, i.e. $\mu_\Delta\left(F_l\left(F_u(M,R),K\right)\right)$. Note that $R(z)=q(z)z^{-N}$ is the kernel of the repetitive controller.

3.4 Effect of nominal angular velocity variation on temporal-based repetitive control

A repetitive control system creates comb-like notches in the system sensitivity function at periodic disturbance frequencies. For a motor/gear rotary system where significant disturbance sources come from gear eccentricity or tooth profile error, temporal frequencies of those disturbances will be proportional to the nominal angular velocity. Thus the performance of temporal-based repetitive control systems will deteriorate as the nominal

angular velocity varies. The velocity variation can be caused by friction, which is usually time-varying and difficult to be taken into account during design of the controller. Based on the proposed TDOF repetitive controller design, Fig. 3 shows the effect of nominal velocity variation on the performance of the sensitivity reduction. Parameters of the repetitive controller were specified to reject a disturbance located at 16 Hz when the system is operating at a nominal angular velocity of 3.14 rad/s. It can be seen that as the nominal velocity deviates from the desired value, the ability of the repetitive controller to reject the disturbance at 16 Hz degrades significantly. As shown in Fig. 3, a 0.2% variation in the nominal speed has an order of magnitude effect in the effectiveness of disturbance rejection. This high sensitivity to operating velocity is the motivation for pursuing the spatial-based repetitive control.

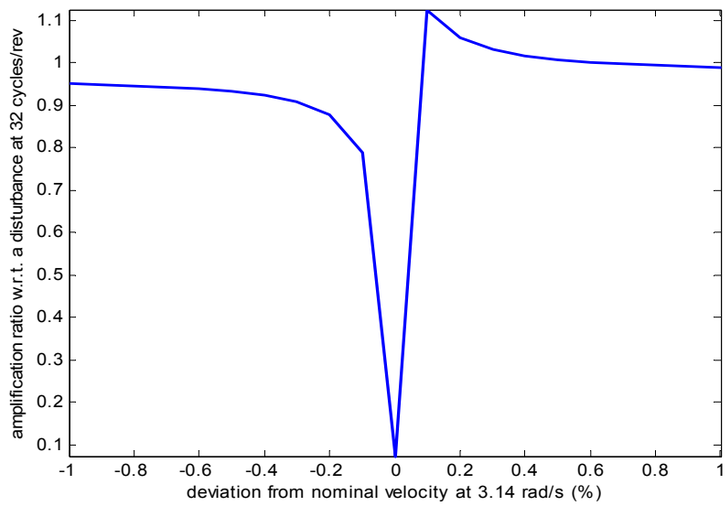

Fig. 3. Effect of nominal angular velocity variation on performance of the repetitive controller.

3.5 Spatial-based repetitive control

The proposed discrete-position repetitive controller was implemented on a typical 600-dpi laser printing system. An optical encoder was mounted on the main rotary component, i.e., an organic photoconductor (OPC) drum. A spatial sampling scheme that uses the encoder pulses (instead of a master clock) to trigger the interrupt of the control algorithm at intervals of equal angular position was implemented. Instead of counting number of pulses within a sampling period, the angular velocity was determined by monitoring the amount of time elapsed for fixed number of encoder pulses. This method actually enables low-cost encoders to achieve high-resolution velocity measurement. The spatial sampling frequency was set at 2000 samples/rev such that the discrete-position repetitive controller has a period of N=2000/16=125. The engine started printing when velocity data of 10 revolutions were collected from the OPC drum for analysis. Fig. 4 shows the measured angular velocity from the OPC drum. Note that as the paper goes through the printing process, it slightly increased the load on the transmission system. This impact decreased the nominal angular velocity from 3.14 rad/s to 3.07 rad/s. However, the frequency spectrums, as shown in Fig. 5, indicated that the performance of the discrete-position repetitive control system was not

degraded by this variation in the nominal velocity. Fig. 5 also shows that capability of the temporal-based repetitive controller was compromised due to frequency shifting of those periodic disturbances.

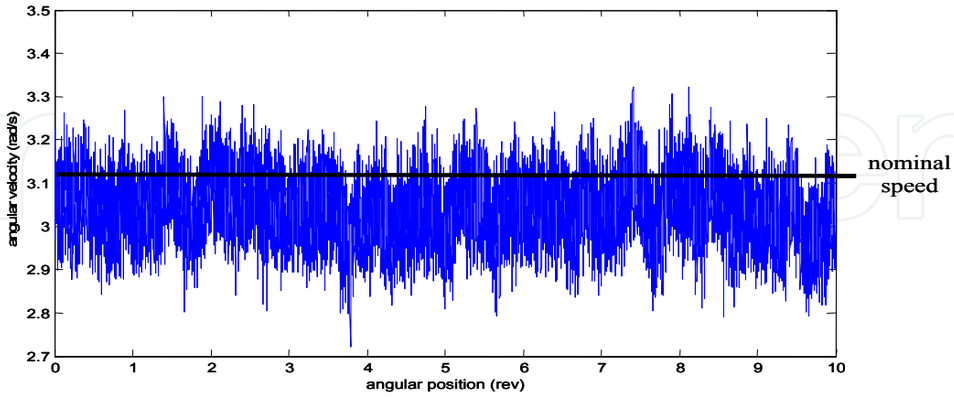

Fig. 4. Measured OPC angular velocity during printing.

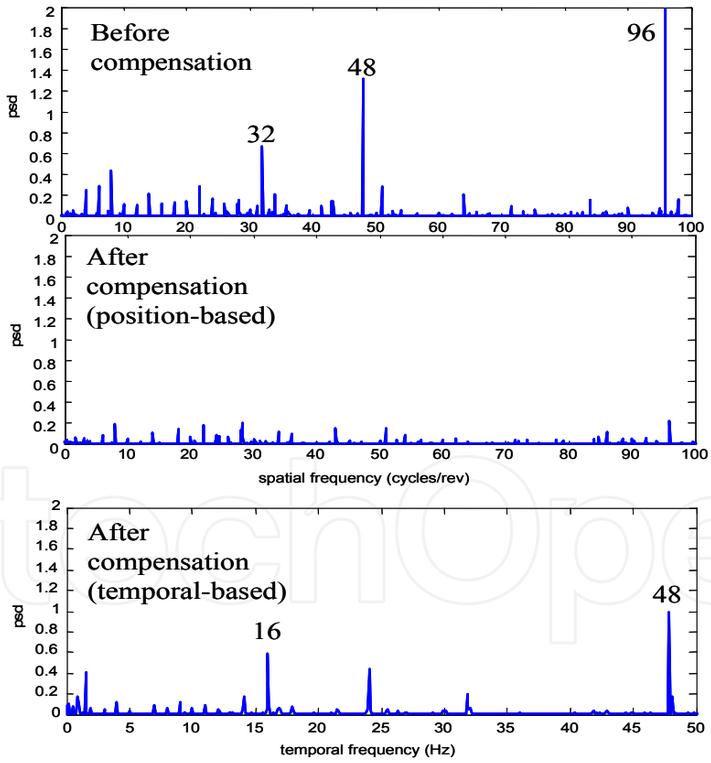

Fig. 5. Experimental PC velocity variation spectrum.

4. Linear parameter varying spatially sampled repetitive control

Several controller design approaches, e.g., design by linearization as shown previously and design for linear periodic system using the lifting technique (Chen & Francis, 1995; Hanson

& Tsao, 2000), can be considered for the ADR system represented in (6). In this section, we first demonstrate that the ADR system with actuator saturation can be formulated into a linear parameter varying (LPV) system. Next, we show that with additional parameterization, LPV gain-scheduling controller synthesis methods (Becker & Packard, 1994; Apkarian et al., 1995) can be applied to the ADR system. Finally, repetitive control and anti-windup (Wu et al., 2000) formulations can be incorporated into the LPV framework to reject spatially periodic disturbances and avoid actuator saturation.

4.1 State-dependent linear parameter varying (LPV) system

Assume that the angular velocity described by (5) can be measured in real-time and the input $\tilde{u}$ and the output $sat(\tilde{u})$ of the actuator saturation is accessible. By defining two varying parameters

$$\rho = \frac{1}{\tilde{\omega}} \text{ and } \phi = \frac{sat(\tilde{u})}{\tilde{u}},$$

we can rewrite (6) as

$$\begin{bmatrix} \dot{\tilde{x}}(\theta) \\ \tilde{z}(\theta) \\ \tilde{y}(\theta) \end{bmatrix} = \left[\begin{array}{c|cc} \tilde{A}(\rho) & \tilde{B}_v(\rho) & \tilde{B}_u(\rho,\phi) \\ \hline C_z & D_{zv} & \tilde{D}_{zu}(\phi) \\ C_y & D_{yv} & 0 \end{array}\right] \begin{bmatrix} \tilde{x}(\theta) \\ \tilde{v}(\theta) \\ \tilde{u}(\theta) \end{bmatrix} \tag{15}$$

where

$$\begin{aligned} &\tilde{A}(\rho) = A\rho, \\ &\tilde{B}_v(\rho) = B_v\rho,\ \tilde{B}_u(\rho,\phi) = B_u\rho\phi, \text{ and} \\ &\tilde{D}_{zu}(\phi) = D_{zu}\phi. \end{aligned}$$

Equation (15) represents a linear parameter-varying (LPV) system with two varying parameters whose values are accessible in real-time. Strictly speaking, (15) represents a quasi-LPV system since one of the varying parameters (ρ) is a function of the system states (Shamma & Athans, 1992).

Without the actuator saturation constraint, i.e. $\phi = 1$, (15) can be written as an affine LPV system,

$$\begin{bmatrix} \dot{\tilde{x}}(\theta) \\ \tilde{z}(\theta) \\ \tilde{y}(\theta) \end{bmatrix} = \left[\begin{array}{c|cc} A\rho & B_v\rho & B_u\rho \\ \hline C_z & D_{zv} & D_{zu} \\ C_y & D_{yv} & 0 \end{array}\right] \begin{bmatrix} \tilde{x}(\theta) \\ \tilde{v}(\theta) \\ \tilde{u}(\theta) \end{bmatrix}. \tag{16}$$

Affine LPV representation has many desirable properties that can facilitate subsequent controller design. For the quasi-LPV system represented by (15), by defining an augmented varying parameter

$$\eta = \rho\phi$$

such that $\tilde{B}_u(\rho,\phi) = B_u\rho\phi = B_u\eta$, (15) can be represented by a pseudo-affine LPV system with three varying parameters (ρ, ϕ, η), i.e.,

$$\begin{bmatrix} \dot{\tilde{x}}(\theta) \\ \tilde{z}(\theta) \\ \tilde{y}(\theta) \end{bmatrix} = \left[\begin{array}{c|cc} \tilde{A}(\rho) & \tilde{B}_v(\rho) & \tilde{B}_u(\eta) \\ \hline C_z & D_{zv} & \tilde{D}_{zu}(\phi) \\ C_y & D_{yv} & 0 \end{array}\right] \begin{bmatrix} \tilde{x}(\theta) \\ \tilde{v}(\theta) \\ \tilde{u}(\theta) \end{bmatrix}. \tag{17}$$

The name pseudo-affine is used since η is not an independent parameter but depends on the other two parameters ρ and ϕ. The impact of over-parameterizing the parameter space will be discussed in later section. Controller synthesis problem for a pseudo-affine LPV system (17) or an affine LPV system (16) can be reduced to solving a finite set of linear matrix inequalities (LMIs) under conditions satisfied by the parameter variation set and the input/output matrices.

The following example demonstrates the process of reformulating a simple 2nd order motor system model to a pseudo-affine LPV system in the angular displacement domain. Consider a transfer function representation of an LTI model for a permanent magnet brushless dc motor,

$$Z(s) = Y(s) + V(s) = \frac{c}{s^2 + as + b}U(s) + V(s), \tag{18}$$

where $U(s)$ is the voltage input to the motor, $V(s)$ is the output disturbance, and $Y(s)$ and $Z(s)$ are the undisturbed and disturbed angular position output, respectively. A state space model for (18) can be obtained by defining a set of state variables $\begin{bmatrix} x_1(t) & x_2(t) \end{bmatrix}^T = \begin{bmatrix} y(t) & \dot{y}(t) \end{bmatrix}^T$, i.e.,

$$\begin{bmatrix} \dot{x}_1(t) \\ \dot{x}_2(t) \\ z(t) \\ y(t) \end{bmatrix} = \left[\begin{array}{cc|cc} 0 & 1 & 0 & 0 \\ -b & -a & 0 & c \\ \hline 1 & 0 & 1 & 0 \\ 1 & 0 & 0 & 0 \end{array}\right] \begin{bmatrix} x_1(t) \\ x_2(t) \\ v(t) \\ sat(u(t)) \end{bmatrix}. \tag{19}$$

Since

$$\begin{bmatrix} \dot{x}_1(t) \\ \dot{x}_2(t) \end{bmatrix} = \frac{d\theta(t)}{dt}\begin{bmatrix} \dot{\tilde{x}}_1(\theta) \\ \dot{\tilde{x}}_2(\theta) \end{bmatrix} = \omega(t)\begin{bmatrix} \dot{\tilde{x}}_1(\theta) \\ \dot{\tilde{x}}_1(\theta) \end{bmatrix},$$

where $\theta(t)$ and $\omega(t)$ are the motor angular position and angular velocity, respectively. We can represent (19) as an ADR pseudo-affine LPV system by defining three varying parameters,

$$\rho = 1/\tilde{\omega}(\theta)\,,\ \phi = sat(\tilde{u})/\tilde{u}\ \text{, and}\ \eta = \rho\phi\,.$$

From (17), the associated LPV system can be written as

$$\begin{bmatrix} \dot{\tilde{x}}_1(\theta) \\ \dot{\tilde{x}}_2(\theta) \\ \tilde{z}(\theta) \\ \tilde{y}(\theta) \end{bmatrix} = \left[\begin{array}{cc|cc} 0 & \rho & 0 & 0 \\ -\rho b & -\rho a & 0 & \eta c \\ \hline 1 & 0 & 1 & 0 \\ 1 & 0 & 0 & 0 \end{array}\right] \begin{bmatrix} \tilde{x}_1(\theta) \\ \tilde{x}_2(\theta) \\ \tilde{v}(\theta) \\ \tilde{u}(\theta) \end{bmatrix}.$$

4.2 Synthesis of gain-scheduling controller for an affine LPV system

We will briefly summarize the results pertinent to the synthesis of an LPV gain-scheduling controller. Note that these results are originally derived for time-based systems, i.e., using time as the independent variable. However, they are equally applicable for an ADR system using angular displacement as the independent variable.

For the LPV system represented by (17), suppose a parameter-dependent output feedback dynamic controller is to be designed from $\tilde{y}$ to $\tilde{u}$, represented by

$$\begin{bmatrix} \dot{\tilde{x}}_K(\theta) \\ \tilde{u}(\theta) \end{bmatrix} = \begin{bmatrix} \tilde{A}_K(\psi) & \tilde{B}_K(\psi) \\ \tilde{C}_K(\psi) & \tilde{D}_K(\psi) \end{bmatrix} \begin{bmatrix} \tilde{x}_K \\ \tilde{y} \end{bmatrix}, \tag{20}$$

where $\psi = (\rho, \phi, \eta)$ forms a parameter vector. Equation (20) is a full-order design in the sense that $\tilde{x} \in R^n$ implies $\tilde{x}_K \in R^n$. Note that the controller is parameterized by the measurable but varying parameter vector ψ, which explains the gain-scheduling characteristics. Define $\tilde{x}_{cl} = \begin{bmatrix} \tilde{x} & \tilde{x}_K \end{bmatrix}^T$, the closed-loop LPV system with (17) and (20) can be expressed as

$$\begin{bmatrix} \dot{\tilde{x}}_{cl}(\theta) \\ \tilde{z}(\theta) \end{bmatrix} = \begin{bmatrix} \tilde{A}_{cl}(\psi) & \tilde{B}_{cl}(\psi) \\ \tilde{C}_{cl}(\psi) & \tilde{D}_{cl}(\psi) \end{bmatrix} \begin{bmatrix} \tilde{x}_{cl}(\theta) \\ \tilde{v}(\theta) \end{bmatrix},$$

where

$$\begin{bmatrix} \tilde{A}_{cl}(\psi) & \tilde{B}_{cl}(\psi) \\ \tilde{C}_{cl}(\psi) & \tilde{D}_{cl}(\psi) \end{bmatrix} = \left[\begin{array}{cc|c} \tilde{A}(\rho) + \tilde{B}_u(\eta)\tilde{D}_K(\psi)C_y & \tilde{B}_u(\eta)\tilde{C}_K(\psi) & \tilde{B}_v(\rho) + \tilde{B}_u(\eta)\tilde{D}_K(\psi)D_{yv} \\ \tilde{B}_K(\psi)C_y & \tilde{A}_K(\psi) & \tilde{B}_K(\psi)D_{yv} \\ \hline \tilde{C}_z(\rho) + \tilde{D}_{zu}(\phi)\tilde{D}_K(\psi)C_y & \tilde{D}_{zu}(\phi)\tilde{C}_K(\psi) & D_{zv} + \tilde{D}_{zu}(\phi)\tilde{D}_K(\psi)D_{yv} \end{array}\right]$$

$$= \left[\begin{array}{cc|c} \tilde{A}(\rho) & 0 & \tilde{B}_v(\rho) \\ 0 & 0 & 0 \\ \hline \tilde{C}_z(\rho) & 0 & D_{zv} \end{array}\right] + \left[\begin{array}{c|c} 0 & \tilde{B}_u(\eta) \\ I & 0 \\ \hline 0 & \tilde{D}_{zu}(\phi) \end{array}\right] \begin{bmatrix} \tilde{A}_K(\psi) & \tilde{B}_K(\psi) \\ \tilde{C}_K(\psi) & \tilde{D}_K(\psi) \end{bmatrix} \left[\begin{array}{cc|c} 0 & I & 0 \\ C_y & 0 & D_{yv} \end{array}\right].$$

In the above equations, all I's and 0's are identity and zero matrices, respectively, with compatible dimensions for block matrix addition and multiplication. Denote the above LPV closed-loop system as P_{cl}. Define the Laplace transform of a signal $\tilde{g}(\theta)$ in the angular displacement domain to be

$$G(\tilde{s}) = \int_0^\infty \tilde{g}(\theta) e^{-\tilde{s}\theta} d\theta .$$

The quadratic LPV γ-performance problem can be summarized in the following theorem:

Theorem 3.1 The LPV closed-loop system P_{cl} is exponentially stable and the scaled H_∞ norm of the system is less than a scalar $\gamma > 0$, i.e.,

$$\left\| L^{1/2} P_{cl} L^{-1/2} \right\|_\infty = \left\| L^{1/2} \tilde{C}_{cl}(\psi)(\tilde{s}I - \tilde{A}_{cl}(\psi))^{-1} \tilde{B}_{cl}(\psi) + \tilde{D}_{cl}(\psi) L^{-1/2} \right\|_\infty < \gamma, \tag{21}$$

for all ψ belonging to a parameter variation set Ψ, if there exists a symmetric positive definite matrix $X \in \mathbf{R}^{n \times n}$ and a scaling matrix L reflecting certain parameter structure such that

$$\begin{bmatrix} \tilde{A}_{cl}^T(\psi)X + X\tilde{A}_{cl}(\psi) & X\tilde{B}_{cl}(\psi) & \tilde{C}_{cl}^T(\psi) \\ \tilde{B}_{cl}^T(\psi)X & -\gamma L & \tilde{D}_{cl}^T(\psi) \\ \tilde{C}_{cl}(\psi) & \tilde{D}_{cl}(\psi) & -\gamma L^{-1} \end{bmatrix} < 0 \tag{22}$$

Proof: See (Becker & Packard, 1994) or (Gahinet & Apkarian, 1994).

With the help of the projection lemma and the completion lemma, the following theorem can be derived to provide the necessary and sufficient conditions for the solvability of the (quadratic) LPV γ-performance problem stated above.

Theorem 3.2 For a given $\psi \in \Psi$, let $N_R(\psi)$ and $N_S(\psi)$ denote orthonormal bases of the null spaces of $\begin{bmatrix} \tilde{B}_u^T(\psi) & \tilde{D}_{zu}^T(\psi) \end{bmatrix}$ and $\begin{bmatrix} \tilde{C}_y(\psi) & \tilde{D}_{yv}(\psi) \end{bmatrix}$, respectively. The LPV γ-performance problem is solvable if and only if there exist symmetric matrices $(R, S) \in \mathbf{R}^{n \times n}$ and symmetric scaling matrices L and J such that the following matrix inequalities

$$\begin{bmatrix} N_R(\psi) & 0 \\ 0 & I \end{bmatrix}^T \left[\begin{array}{cc|c} \tilde{A}(\psi)R + R\tilde{A}^T(\psi) & R\tilde{C}_z^T(\psi) & \tilde{B}_v(\psi) \\ \tilde{C}_z(\psi)R & -\gamma J & \tilde{D}_{zv}(\psi) \\ \hline \tilde{B}_v^T(\psi) & \tilde{D}_{zv}^T(\psi) & -\gamma L \end{array}\right] \begin{bmatrix} N_R(\psi) & 0 \\ 0 & I \end{bmatrix} < 0, \tag{23}$$

$$\begin{bmatrix} N_S(\psi) & 0 \\ 0 & I \end{bmatrix}^T \left[\begin{array}{cc|c} \tilde{A}^T(\psi)S + S\tilde{A}(\psi) & S\tilde{B}_v(\psi) & \tilde{C}_z^T(\psi) \\ \tilde{B}_v^T(\psi)S & -\gamma J & \tilde{D}_{zv}^T(\psi) \\ \hline \tilde{C}_z(\psi) & \tilde{D}_{zv}(\psi) & -\gamma L \end{array}\right] \begin{bmatrix} N_S(\psi) & 0 \\ 0 & I \end{bmatrix} < 0, \tag{24}$$

$$\begin{bmatrix} R & I \\ I & S \end{bmatrix} \geq 0 \tag{25}$$

$$LJ = I \tag{26}$$

hold for all $\psi \in \Psi$.

Proof: Follows the proof in the appendix of (Gahinet & Apkarian, 1995). The only difference being that most matrices are now parameter dependent.

If the LPV γ-performance problem is solvable, the two symmetric matrices R and S along with the value of γ and the system matrices ($\tilde{A}(\psi)$, $\tilde{B}_v(\psi)$, $\tilde{B}_u(\psi)$, etc.) can be used to synthesize the controller matrices ($\tilde{A}_K(\psi)$, $\tilde{B}_K(\psi)$, $\tilde{C}_K(\psi)$, and $\tilde{D}_K(\psi)$) (Becker & Packard, 1994; Gahinet, 1996).

Remark The scaling matrix L in the above theorems takes into account the structural information on the mapping relating input $\tilde{v}$ and output $\tilde{z}$ in (17), which can include unmodeled dynamics, errors in sensing the varying parameters, and uncertain parameters which can not be measured in real-time. However, the resulting matrix inequalities are nonconvex, mainly due to (26), and computational techniques such as scaling/controller iteration or D/K iteration will be required to solve for matrices R and S.

To simplify the subsequent derivation, we will be conservative and ignore the structural information of the mapping between $\tilde{v}$ and $\tilde{z}$. This is equivalent to setting $L = J = I$ and removing the constraint defined by (26) from the above theorem. The advantage of doing so is that (23)-(25) become LMIs in R and S and the optimization becomes a convex problem that can be solved using numerical solvers based on interior point method, e.g., (Gainet et al., 1995). To check the solvability of the problem for the system given by (17) using Theorem 3.2, the following substitution is used

$$\begin{aligned}
&\tilde{A}(\psi) = A\rho,\ \tilde{B}_v(\psi) = B_v\rho,\ \tilde{B}_u(\psi) = B_u\eta,\\
&\tilde{C}_z(\psi) = C_z,\ \tilde{D}_{zv}(\psi) = D_{zv},\ \tilde{D}_{zu}(\psi) = \tilde{D}_{zu}(\phi),\\
&\tilde{C}_y(\psi) = C_y,\ \tilde{D}_{yv}(\psi) = D_{yv}.
\end{aligned}$$

Since Ψ constitutes infinite number of elements, inequalities (23)-(25) pose solvability issue with infinite number of LMI constraints. It was suggested in (Becker & Packard, 1994) that the parameter space be gridded and a controller is synthesized such that it satisfies the solvability conditions at the finite number of parameter values. However, for fixed grid spacing, the number of grid points grows rapidly as the number of parameters increases. Another way to reduce the number of constraints is to take advantage of the properties of polytopic LPV systems.

Definition An LPV system is polytopic if the state-space matrices of the system depend affinely on the varying parameters that lie within a polytope, i.e.,

$$\psi \in \Psi = \left\{ \sum_{i=1}^{r} \alpha_i \psi_i : \sum_{i=1}^{r} \alpha_i = 1,\ \alpha_i \geq 0 \right\},$$

where r is the number of vertices of the polytope and ψ_i is the parameter vector corresponding to a vertex of the polytope.

Proposition Let $f : \prod \to \mathbf{R}$ be a convex function where $\prod$ is a convex set with vertices π_i's, i.e., $\Pi = \left\{ \sum_{i=1}^{r} \alpha_i \pi_i : \sum_{i=1}^{r} \alpha_i = 1,\ \alpha_i \geq 0 \right\}$. Then $f(x) < \gamma$ for all $x \in \prod$ if and only if $f(\pi_i) < \gamma$ for i=1, 2,…, r (Berkovitz, 2002).

For a polytopic LPV system satisfying the following two assumptions:

i. $\tilde{D}_{yu}(\psi) = 0$; that is, no direct transmission from $\tilde{u}$ to $\tilde{y}$,

ii. $\tilde{B}_u(\psi) = \tilde{B}_u$, $\tilde{C}_y(\psi) = \tilde{C}_y$, $\tilde{D}_{zu}(\psi) = \tilde{D}_{zu}$, and $\tilde{D}_{yv}(\psi) = \tilde{D}_{yv}$; that is, those matrices are constant matrices that are independent of the varying parameters,

it can be easily shown (using the above proposition) that (23) and (24) in Theorem 3.2 hold if and only if they hold for the matrices corresponding to the vertices of the parameter polytope, i.e., $\tilde{A}(\psi_i)$, $\tilde{B}_v(\psi_i)$, $\tilde{C}_z(\psi_i)$, $\tilde{D}_{zv}(\psi_i)$ for i=1, 2,…, r (Apkarian et al., 1995). In other

words, only the $2r+1$ LMIs corresponding to the vertices of the parameter polytope need to be formed for solving matrices R and S in Theorem 3.2.

The affine-LPV system represented in (16) qualifies as a polytopic system with matrix $\tilde{D}_{yu}=0$ and the matrices $A\rho$, $B_v\rho$, and $B_u\rho$ depend on the varying parameter ρ. Although the pseudo-affine LPV system represented by (17) has similar structure as (16) with $\tilde{D}_{yu}=0$ and the matrices $\tilde{A}$, $\tilde{B}_v$, $\tilde{B}_u$, and $\tilde{D}_{zu}$ depend on varying parameters, it is not polytopic due to the dependency of the varying parameter η on the two varying parameters ρ and ϕ. In such cases, a polytope can usually be found to bound and replace the parameter variation set. To satisfy the assumption (ii), parameter dependency of the $\tilde{B}_u$ or the $B_u\rho$ matrix can be removed by filtering the input channel, as will be discussed in section 3.3. For systems without direct transmission between $\tilde{u}$ and $\tilde{z}$, e.g. the brushless dc motor system demonstrated in section 3.1, it is easy to verify that $\tilde{D}_{zu}=D_{zu}=0$.

4.3 Incorporating spatial-sampled repetitive control and actuator anti-windup

The overall control structure is summarized in Fig. 6. Here $G(\psi)$ along with the actuator saturation block represents the pseudo-affine LPV system, Δ denotes the modeling uncertainty, and W_1 and W_2 are weighting filters whose frequency-dependent magnitudes are used to bound the performance specifications and model uncertainty. The repetitive controller is denoted by RC and the LPV controller to be designed is denoted by $K(\psi)$. The open-loop LPV system (within the dashed-line block in Fig. 6) can be expressed as

$$\begin{bmatrix}\dot{\tilde{x}}(\theta)\\ \tilde{q}(\theta)\\ \tilde{z}(\theta)\\ \tilde{y}(\theta)\end{bmatrix}=\left[\begin{array}{c|ccc}\tilde{A}(\rho) & \tilde{B}_p(\rho) & \tilde{B}_v(\rho) & \tilde{B}_u(\eta)\\ \hline C_q & D_{qp} & D_{qv} & \tilde{D}_{qu}(\phi)\\ C_z & D_{zp} & D_{zv} & \tilde{D}_{zu}(\phi)\\ C_y & D_{yp} & D_{yv} & 0\end{array}\right]\begin{bmatrix}\tilde{x}(\theta)\\ \tilde{p}(\theta)\\ \tilde{v}(\theta)\\ \tilde{u}(\theta)\end{bmatrix}, \tag{27}$$

which differs from (17) in that unstructured model uncertainty, connecting output $\tilde{q}$ to input $\tilde{p}$, and weighting filters are also incorporated. The current formulation considers two types of perturbations. One is due to the varying parameters, which is bounded and can be measured in real-time. The other is due to modeling error, which is also bounded but can not be measured in real-time. In (27), without actuator saturation constraint, i.e. $\phi=1$, we have $\eta=\rho$ and the matrices $\tilde{D}_{qu}$ and $\tilde{D}_{zu}$ become constant matrices and independent of varying parameters.

To account for spatially periodic disturbances, we will consider a low-order and attenuated spatial-based repetitive controller that takes the form of

$$RC(\tilde{s})=\frac{1}{\tilde{s}/\omega_r+1}\prod_{i=1}^{k}\frac{\tilde{s}^2+2\zeta_i\omega_{ni}\tilde{s}+\omega_{ni}^2}{\tilde{s}^2+2\xi_i\omega_{ni}\tilde{s}+\omega_{ni}^2}$$

or equivalently in state space representation

$$\begin{aligned}\dot{\tilde{x}}_{rc}&=A_{rc}\tilde{x}_{rc}+B_{rc}\tilde{y}\\ \tilde{y}_2&=C_{rc}\tilde{x}_{rc}\end{aligned},$$

where k is the number of spatially sinusoidal disturbances that is to be compensated. ω_{ni} is the i^{th} disturbance frequency in rad/rev. Damping ratios associated with the poles, ζ_i, and zeros, ξ_i, of the repetitive filter need to satisfy the condition $0 < \xi_i < \zeta_i < 1$, to ensure sensitivity reduction at spatial frequency ω_{ni} rad/rev. The gain of the repetitive controller $RC(\tilde{s})$ can be adjusted by varying ξ_i and ζ_i. A low-pass filter with roll-off frequency ω_r rad/rev is included to attenuate the controller gain in the high frequency region that is similar to the q-filter used in a digital repetitive controller. As shown in Fig. 6, the repetitive controller takes $\tilde{y}$ as input and creates a new input $\tilde{y}_2$ to the 'to-be-designed' LPV controller $K(\psi)$.

To address actuator saturation, an anti-windup scheme as proposed in [36] can be formulated that feeds the difference between the actuator input and output back to the controller. This corresponds to creating a new input for the LPV controller, i.e.,

$$\tilde{y}_1 = (\phi - 1)\tilde{u}.$$

If the control $\tilde{u}$ does not saturate, i.e., $\phi = 1$, then $\tilde{y}_1 = 0$ and this additional input is deactivated. If the control $\tilde{u}$ saturates, i.e., $\phi < 1$, then $\tilde{y}_1 \neq 0$, which provides additional degree of freedom for manipulating the control $\tilde{u}$.

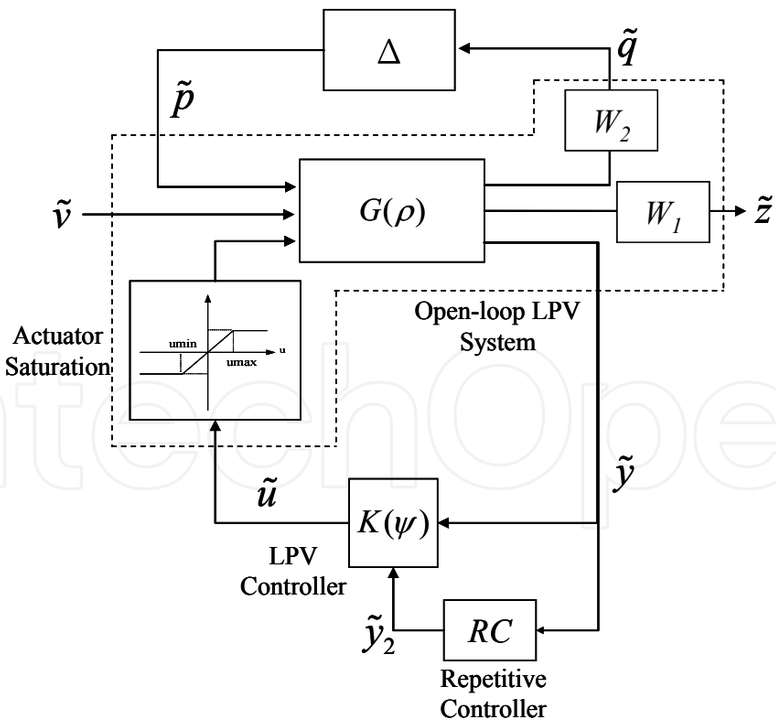

Fig. 6. LPV gain-scheduling control system with repetitive controller.

The open-loop LPV system with repetitive and anti-windup control (within the dashed-line block in Fig. 6) can be shown to have the following state-space representation:

$$\begin{bmatrix} \dot{\tilde{x}}(\theta) \\ \dot{\tilde{x}}_{rc}(\theta) \\ \tilde{q}(\theta) \\ \tilde{z}(\theta) \\ \tilde{y}(\theta) \\ \tilde{y}_1(\theta) \\ \tilde{y}_2(\theta) \end{bmatrix} = \left[\begin{array}{cc|ccc} \tilde{A}(\rho) & 0 & \tilde{B}_p(\rho) & \tilde{B}_v(\rho) & \tilde{B}_u(\eta) \\ B_{rc}C_y & A_{rc} & B_{rc}D_{yp} & B_{rc}D_{yv} & 0 \\ \hline C_q & 0 & D_{qp} & D_{qv} & \tilde{D}_{qu}(\phi) \\ C_z & 0 & D_{zp} & D_{zv} & \tilde{D}_{zu}(\phi) \\ C_y & 0 & D_{yp} & D_{yv} & 0 \\ 0 & 0 & 0 & 0 & \phi - 1 \\ 0 & C_{rc} & 0 & 0 & 0 \end{array}\right] \begin{bmatrix} \tilde{x}(\theta) \\ \tilde{x}_{rc}(\theta) \\ \tilde{p}(\theta) \\ \tilde{v}(\theta) \\ \tilde{u}(\theta) \end{bmatrix}. \tag{28}$$

Note that the LPV controller $K(\psi)$ now has three inputs $(\tilde{y}, \tilde{y}_1, \tilde{y}_2)$ and one output $\tilde{u}$. The parameter dependency of the input and output matrices (e.g., $\tilde{B}_u$ and C_y), if any, can be removed by considering the dynamics of the sensors and actuators (Apkarian et al., 1995). Let

$$\begin{bmatrix} \dot{\tilde{x}}_{o1} \\ \dot{\tilde{x}}_{o2} \\ \dot{\tilde{x}}_{o3} \end{bmatrix} = \begin{bmatrix} A_{o1} & 0 & 0 \\ 0 & A_{o2} & 0 \\ 0 & 0 & A_{o3} \end{bmatrix} \begin{bmatrix} \tilde{x}_{o1} \\ \tilde{x}_{o2} \\ \tilde{x}_{o3} \end{bmatrix} + \begin{bmatrix} B_{o1} & 0 & 0 \\ 0 & B_{o2} & 0 \\ 0 & 0 & B_{o3} \end{bmatrix} \begin{bmatrix} \tilde{y} \\ \tilde{y}_1 \\ \tilde{y}_2 \end{bmatrix},$$

$$\begin{bmatrix} \hat{y} \\ \hat{y}_1 \\ \hat{y}_2 \end{bmatrix} = \begin{bmatrix} C_{o1} & 0 & 0 \\ 0 & C_{o2} & 0 \\ 0 & 0 & C_{o3} \end{bmatrix} \begin{bmatrix} \tilde{x}_{o1} \\ \tilde{x}_{o2} \\ \tilde{x}_{o3} \end{bmatrix},$$

where $(\hat{y}, \hat{y}_1, \hat{y}_2)$ represent the new outputs, and

$$\begin{aligned} \dot{\tilde{x}}_i &= A_i \tilde{x}_i + B_i \hat{u}, \\ \tilde{u} &= C_i \tilde{x}_i, \end{aligned}$$

where $\hat{u}$ represent the new input. This action is equivalent to passing each input or output channel of the open-loop LPV system in (28) through a low-pass filter

$$\begin{aligned} H_j(\tilde{s}) &= C_{oj}(\tilde{s}I - A_{oj})^{-1} B_{oj}, \ j = 1,2,3 \text{ or} \\ F(\tilde{s}) &= C_i(\tilde{s}I - A_i)^{-1} B_i \end{aligned},$$

respectively, before connecting to the LPV controller $K(\psi)$, as depicted in Fig. 7. The bandwidth of the low-pass filters depends on the sensor and actuator dynamics. For negligible senor or actuator dynamics, the bandwidth can be assigned to be much larger than that of the open-loop system to minimize possible interference. With the inclusion of the anti-windup formulation and the input/output filters, the overall open-loop LPV system with parameter-free input-output matrices can be found to be

$$\begin{bmatrix} \dot{\tilde{x}}(\theta) \\ \dot{\tilde{x}}_{rc}(\theta) \\ \dot{\tilde{x}}_{o1}(\theta) \\ \dot{\tilde{x}}_{o2}(\theta) \\ \dot{\tilde{x}}_{o3}(\theta) \\ \dot{\tilde{x}}_{i}(\theta) \\ \tilde{q}(\theta) \\ \tilde{z}(\theta) \\ \hat{y}(\theta) \\ \hat{y}_1(\theta) \\ \hat{y}_2(\theta) \end{bmatrix} = \left[\begin{array}{ccccc|c|ccc} \tilde{A}(\rho) & 0 & 0 & 0 & 0 & \tilde{B}_u(\eta)C_i & \tilde{B}_p(\rho) & \tilde{B}_v(\rho) & 0 \\ B_{rc}C_y & A_{rc} & 0 & 0 & 0 & 0 & B_{rc}D_{yp} & B_{rc}D_{yv} & 0 \\ B_{o1}C_y & 0 & A_{o1} & 0 & 0 & 0 & B_{o1}D_{yp} & B_{o1}D_{yv} & 0 \\ 0 & 0 & 0 & A_{o2} & 0 & B_{02}(\phi-1)C_i & 0 & 0 & 0 \\ 0 & B_{o3}C_{rc} & 0 & 0 & A_{o3} & 0 & 0 & 0 & 0 \\ 0 & 0 & 0 & 0 & 0 & A_i & 0 & 0 & B_i \\ \hline C_q & 0 & 0 & 0 & 0 & \tilde{D}_{qu}(\phi)C_i & D_{qp} & D_{qv} & 0 \\ C_z & 0 & 0 & 0 & 0 & \tilde{D}_{zu}(\phi)C_i & D_{zp} & D_{zv} & 0 \\ 0 & 0 & C_{o1} & 0 & 0 & 0 & 0 & 0 & 0 \\ 0 & 0 & 0 & C_{o2} & 0 & 0 & 0 & 0 & 0 \\ 0 & 0 & 0 & 0 & C_{o3} & 0 & 0 & 0 & 0 \end{array}\right] \begin{bmatrix} \tilde{x}(\theta) \\ \tilde{x}_{rc}(\theta) \\ \tilde{x}_{o1}(\theta) \\ \tilde{x}_{o2}(\theta) \\ \tilde{x}_{o3}(\theta) \\ \tilde{x}_{i}(\theta) \\ \tilde{p}(\theta) \\ \tilde{v}(\theta) \\ \hat{u}(\theta) \end{bmatrix}. \quad (29)$$

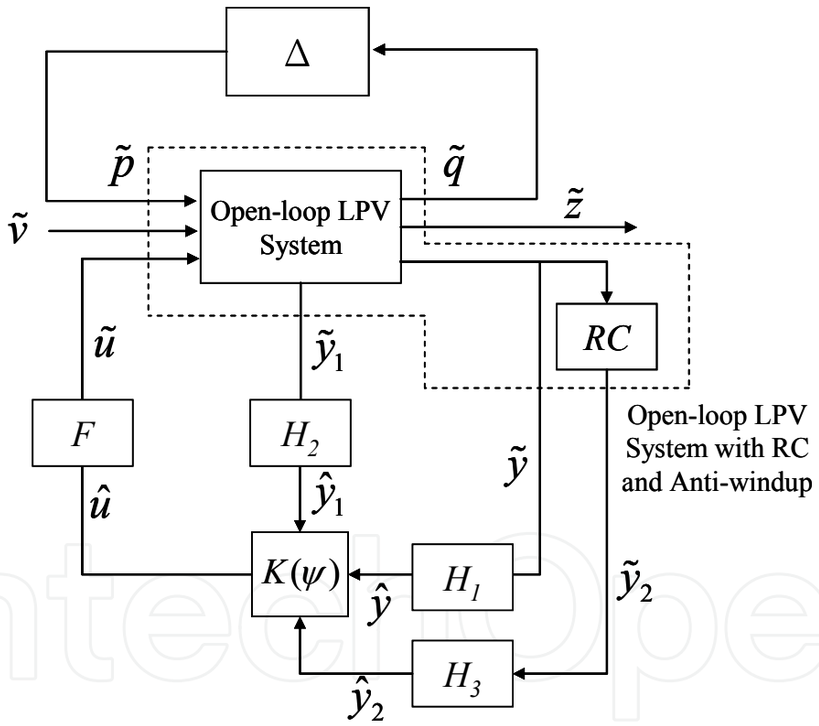

Fig. 7. LPV gain-scheduling control system with repetitive controller, anti-windup scheme, and sensor/actuator dynamics.

By making the following definitions

$$\tilde{X} = \begin{bmatrix} \tilde{x} & \tilde{x}_{rc} & \tilde{x}_{o1} & \tilde{x}_{o2} & \tilde{x}_{o3} & \tilde{x}_i \end{bmatrix}^T,$$
$$\tilde{Z} = \begin{bmatrix} \tilde{q} & \tilde{z} \end{bmatrix}^T,\ \tilde{Y} = \begin{bmatrix} \hat{y} & \hat{y}_1 & \hat{y}_2 \end{bmatrix}^T,\ \tilde{V} = \begin{bmatrix} \tilde{p} & \tilde{v} \end{bmatrix}^T,\ \tilde{U} = \hat{u},$$

we can rewrite the above system as

$$\begin{bmatrix} \dot{\tilde{X}} \\ \tilde{Z} \\ \tilde{Y} \end{bmatrix} = \begin{bmatrix} A(\psi) & B_V(\psi) & B_U \\ C_Z(\psi) & D_{ZV}(\psi) & D_{ZU} \\ C_Y & D_{YV} & 0 \end{bmatrix} \begin{bmatrix} \tilde{X} \\ \tilde{V} \\ \tilde{U} \end{bmatrix}, \tag{30}$$

where the system and input/output matrices are of appropriate dimensions and can be identified from (2). Note that the matrices B_U and C_Y are free of varying parameters.

4.4 Discretization of angular displacement reformulated systems

A spatial sampling scheme that uses the output pulses of an optical shaft encoder (instead of a clock signal) to trigger the interrupt of the control algorithm at intervals of equal angular displacement was implemented. The constant angular displacement based sampling effectively discretized the control system in the angular displacement domain. Note that an ADR system, see (15), without varying parameters can be viewed as an LTI system with angular displacement θ as the independent variable as compared with time t. Theorems or methods used to derive the discrete equivalent of LTI systems, e.g., z-transform (impulse invariant), zero-order hold (step invariant), and bilinear or trapezoid rule, can be applied to ADR systems with slightest modification. What needs to be kept in mind is that the sampling behavior has changed from equal time interval (in sec) to equal angular displacement interval (in revolution).

4.5 Experimental setup and validation

Rotational velocity regulation in a laser printer will be used to verify the effectiveness of the proposed spatially sampled repetitive control in rejecting spatially periodic disturbances. A 600-dpi monochrome laser printer is used as the experimental platform that comprised of one brushless dc motor, with a set of gear and a photosensitive drum. The hardware setup is depicted in Fig. 8. The motor velocity is regulated by adjusting the voltage input to a pulse width modulated (PWM) power drive. A digital encoder with a resolution of 50,000 pulses/rev is mounted on the photosensitive drum to measurement of angular displacement and velocity. To maintain the desired dot placement accuracy, the photosensitive drum is expected to rotate at a nominal angular velocity of 0.5 rev/sec. This corresponds to a motor voltage input of 2.56 volts. The saturation limits for the input voltage are identified to be ±0.5 volts around the nominal value, i.e., $u_{\max} = 3.06$ and $u_{\min} = 2.06$. According to the frequency spectrum of the measured speed fluctuations, spatially periodic components at spaitial frequencies of 32, 48, and 96 cycles/rev need to be reduced, since they caused visible bands in printed images. A 2nd order transfer function from the motor voltage input to the drum angular velocity output is obtained to approximate the actual frequency response of the experimental platform, i.e.

$$P_{yu}(s) = \frac{4.184 \times 10^5}{s^2 + 2246s + 8.932 \times 10^4}.$$

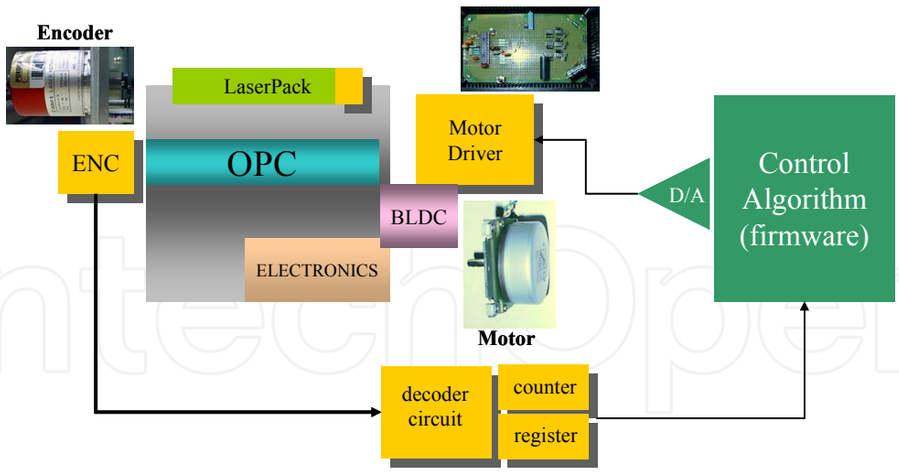

Fig. 8. Experimental setup for the closed-loop control of a typical 600-dpi monochrome laser printer.

The output multiplicative modeling errors are obtained by comparing the frequency responses of the plant model and the experimental platform, as shown in Fig. 9. Note that the spatial frequency response shown in Fig. 9 is obtained from the temporal frequency response where the spatial frequency in cycle per revolution is scaled by the nominal angular velocity. A stable 1st order filter that upper bounds the multiplicative model uncertainty can be found to be

$$W_2(\tilde{s}) = 0.03\frac{\tilde{s}/16+1}{\tilde{s}/700+1}.$$

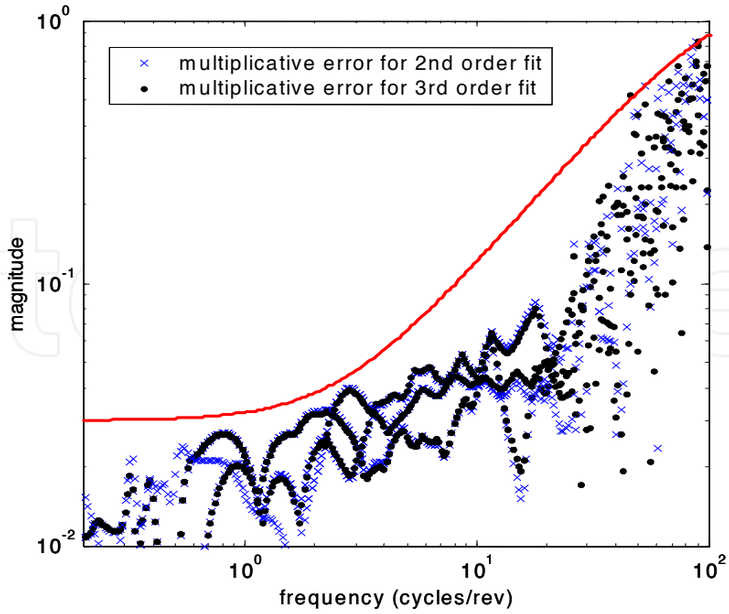

Fig. 9. Output multiplicative uncertainties for the experimental platform approximated using a 2nd or 3rd order transfer function. The solid line is the magnitude of a 1st order filter that upper bounds the uncertainties.

Note that the affine nature of the open-loop LPV system (29) will be intact after inclusion of the parameter independent filter, W_2. The selection of W_1 requires more considerations. First of all, the LPV controller will be independent of the saturation indicator ϕ if the performance weighting does not depend on ϕ [36]. In other words, the design problem using parameter-free W_1 will degenerate to one without actuator saturation. Secondly, if a parameter dependent W_1 filter is chosen, the affine nature of the LPV open-loop system will be preserved after incorporating the filter. Thus, a feasible W_1 filter can assume the following state space realization

$$\dot{\tilde{x}}_{w1} = -(\omega_b\phi + b)\tilde{x}_{w1} + \sqrt{e}\tilde{z},$$
$$\hat{z} = \sqrt{e}\phi\tilde{x}_{w1} + k\tilde{z},$$

which has the transfer function

$$W_1(\tilde{s}) = k + \frac{e\phi}{\tilde{s} + \omega_b\phi + b}.$$

Note that the magnitude curve of W_1 can be specified by tuning the constant values of ω_b, b, e, and k. Specifically, k can be used to specify the lower bound for the W_1 magnitude at high frequencies (i.e., as $\tilde{s} \to \infty$); the coefficient b can be used to specify the lower bound of the corner frequencies; coefficients ω_b and e can be used to specify the exact corner frequencies and the W_1 magnitude at low frequencies (i.e., as $\tilde{s} \to 0$). The parameter variation set $\bar{\Psi}$ is determined to be

$$\bar{\Psi} = \{(\rho, \phi, \eta):\ 1 \le \rho \le 10,\ 0.1 \le \phi \le 1,\ \eta = \rho\phi\}.$$

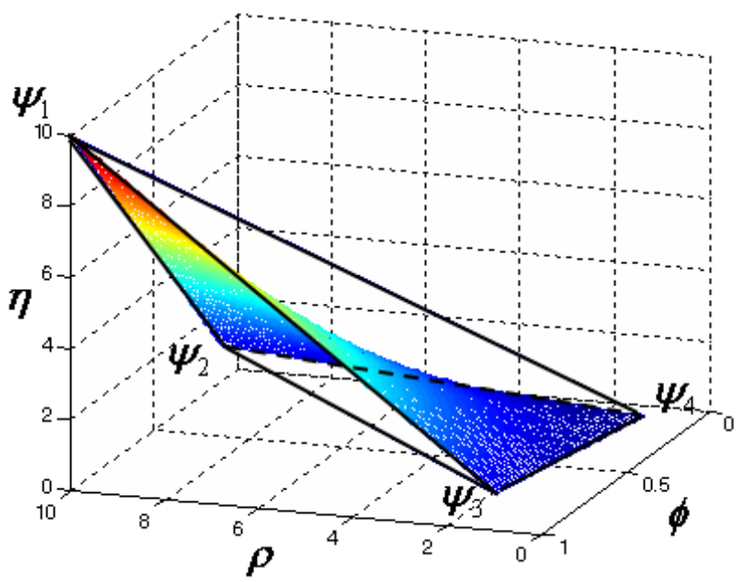

Fig. 10. Parameter variation set $\bar{\Psi}$ and the selected (convex) polytope Ψ which bounds the set.

The upper and lower bounds of ρ and ϕ are empirically determined based on a velocity variation from –80 % to +100% around the nominal value of 0.5 rev/sec and a 10-to-1 saturation limit, respectively. The parameter variation set $\bar{\Psi}$ is not convex but can be shown to lie within a polytope Ψ with four vertices located at $\psi_1 = (10,1,10)$, $\psi_2 = (10,0.1,1)$, $\psi_3 = (1,1,1)$, and $\psi_4 = (1,0.1,0.1)$ (see Fig. 10). The polytope Ψ will be used for the following design. Given that $\phi \in [0.1, 1]$ in Ψ, the parameters of the weighting filter W_1 can be properly determined to reflect the different performance requirement for the unsaturated ($\phi = 1$) and saturated ($\phi < 1$) system. Fig. 11 shows the magnitude curves of W_1 with $k = 0.03$, $\omega_b = 2\pi\times12$, $b = 0.1\omega_b$ and $e=5/3\times\omega_b$ as $\phi \in [0.1, 1]$. The magnitude curve of W_2 is also shown in the figure. The low-pass filters $H_j(\tilde{s})$ and $F(\tilde{s})$ are selected as

$$H_1(\tilde{s}) = H_2(\tilde{s}) = H_3(\tilde{s}) = F(\tilde{s}) = \frac{1}{\tilde{s}/(2\pi\times1000)+1}$$

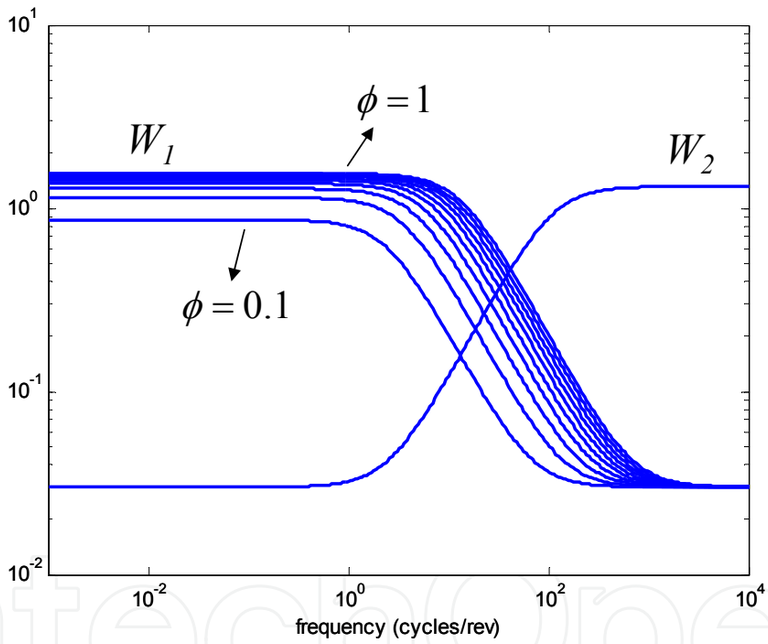

Fig. 11. The parameter-dependent performance weighting W_1 and uncertainty weighting W_2.

where the frequency value of 1000 cycles/rev is specified to reflect the negligible sensor and actuator dynamics. The low-order attenuated repetitive controller can be expressed as

$$RC(\tilde{s}) = \frac{1}{\tilde{s}/(2\pi\times200)+1} \prod_{\substack{\omega_n=32,48,96 \\ \xi_n=0.002,0.002,0.001}} \frac{\tilde{s}^2 + 2\times0.1\times\omega_n\tilde{s} + {\omega_n}^2}{\tilde{s}^2 + 2\times\xi_n\omega_n\tilde{s} + {\omega_n}^2},$$

where the periodic disturbances are at 32, 48 and 96 cycles/rev. A feasible LPV controller is determined based on the above parameters, which attains $\gamma = 1.1669$. The controller can be written as

$$\begin{bmatrix}\dot{\tilde{x}}_K\\ \dot{\tilde{x}}_{rc}\end{bmatrix}=\begin{bmatrix}A_K(\psi) & 0\\ 0 & A_{rc}\end{bmatrix}\begin{bmatrix}\tilde{x}_K\\ \tilde{x}_{rc}\end{bmatrix}+\begin{bmatrix}B_{K1}(\psi) & B_{K2}(\psi) & B_{K3}(\psi) & 0\\ 0 & 0 & 0 & B_{rc}\end{bmatrix}\begin{bmatrix}\hat{y}_1\\ \hat{y}\\ \hat{y}_2\\ \tilde{y}\end{bmatrix}, \tag{31}$$

$$\begin{bmatrix}\hat{u}\\ \tilde{y}_2\end{bmatrix}=\begin{bmatrix}C_K(\psi) & 0\\ 0 & C_{rc}\end{bmatrix}\begin{bmatrix}\tilde{x}_K\\ \tilde{x}_{rc}\end{bmatrix}+\begin{bmatrix}D_{K1}(\psi) & D_{K2}(\psi) & D_{K3}(\psi) & 0\\ 0 & 0 & 0 & 0\end{bmatrix}\begin{bmatrix}\hat{y}_1\\ \hat{y}\\ \hat{y}_2\\ \tilde{y}\end{bmatrix}, \tag{32}$$

where

$$B_K(\psi)=[B_{K1}(\psi)\quad B_{K2}(\psi)\quad B_{K3}(\psi)],$$
$$D_K(\psi)=[D_{K1}(\psi)\quad D_{K2}(\psi)\quad D_{K3}(\psi)].$$
$$\psi=\{\sum_{i=1}^{4}\alpha_i\psi_i:\alpha_i\geq 0,\ \sum_{i=1}^{4}\alpha_i=1\}$$

We can view (31) and (32) as an LPV repetitive controller (LPVRC). For practical implementation, the vertex controllers need to be transformed into their discrete-position invariant counterparts, e.g., using bilinear transformation. The nominal performance (NP), robust stability (RS), and robust performance (RP) curves for the four vertex systems are shown in Fig. 12.

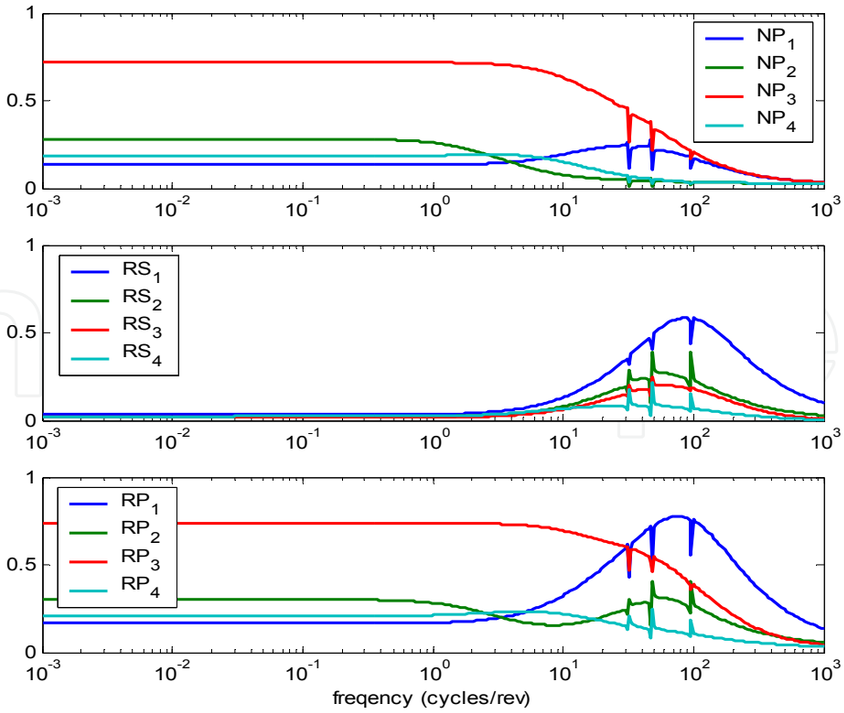

Fig. 12. NP, RS and RP curves for the four vertex closed-loop systems.

The experiment was performed by activating the LPVRC controller and rotating the photosensitive drum for 40 revolutions with step change in nominal velocity. During the operation, the nominal motor input voltage was changed at the 10th, 20th and 30th revolution, which shifted the nominal drum angular velocity. This can be seen in Fig. 13, which depicts the histories of drum angular velocity, motor input voltage and the three varying parameters with respect to the drum angular position. Fig. 14 compares the spatial frequency spectrum of the velocity signals within each 10-revolution interval to that of the uncompensated system. We can see that the performance of the LPVRC controlled system is insensitive to changes in nominal drum angular velocity. Note that the magnitude increases near dc frequency are due to the transient responses. As a comparison, Fig. 15 shows the responses when the system is under the control of a fixed temporal repetitive controller. As expected, a fixed-period repetitive controller operating in the time domain is unable to effectively compensate for the disturbances whose temporal periods change with the rotational speed of the system.

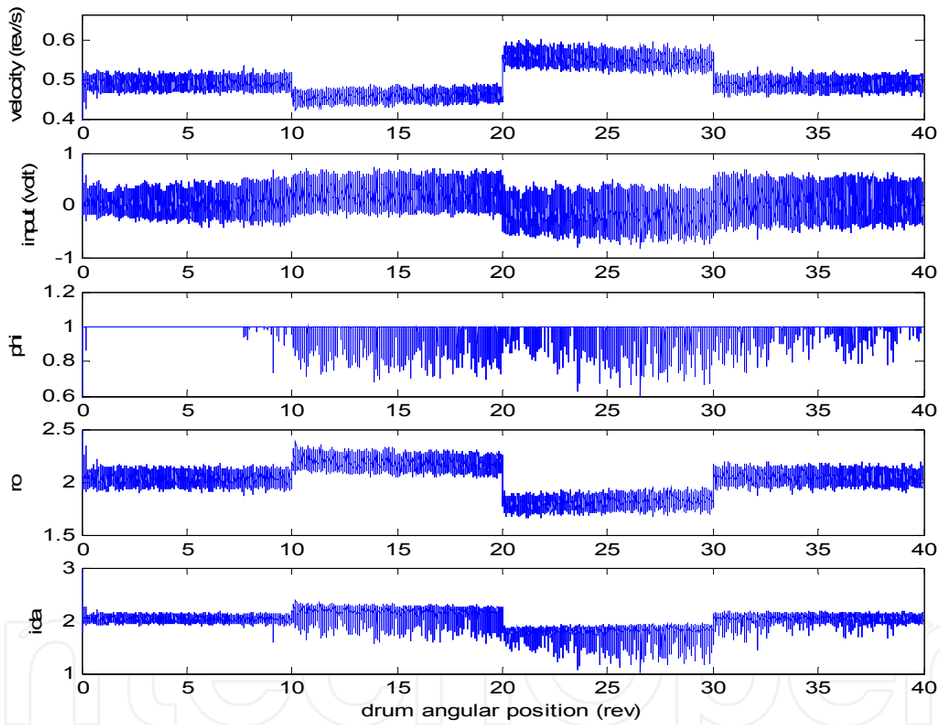

Fig. 13. Histories of drum angular velocity, motor input voltage and the three varying parameters with respect to drum angular position.

The spatial sampling scheme proposed in this section raises a practical issue when synthesizing digital full-order repetitive controllers. The available sampling frequencies when conducting the scheme depends on the encoder resolution. For example, if the resolution of an encoder is 5000 pulses/rev, the highest sampling frequency achievable using the scheme will be 5000 cycles/rev. Other available sampling frequencies, depending on implementable divide-by-N circuits, might be 2500 (when the pulses are divided by 2), 500 (divided by 10), etc. Due to limited choices of sampling frequencies, the number of delay taps N for the repetitive kernel (i.e. q^{-N}), which is the ratio of the sampling frequency and the

disturbance frequency, might end up being non-integral when tackling certain disturbance frequencies.

Other nonlinear control design approaches (e.g., sliding mode and adaptive control) can also be employed. However, it is not clear if frequency-wise tradeoff between performance and stability can be easily performed within those nonlinear design frameworks.

It is also worth mentioning that the LPV gain-scheduling design may encounter the following implementation issues:

i. The state-dependent varying parameters may leave the parameter variation set.
ii. The measurement of the varying parameters may be contaminated by noise.
iii. There may be delay induced in the measurement of the varying parameters.

A feasible solution for the first issue is to setup the parameter variation set more accurately. Note that (22) implies that $\tilde{A}_{cl}^{T}(\psi)X + X\tilde{A}_{cl}(\psi) < 0$, and we can pick a Lyapunov function $V(\tilde{x}_{cl}(\theta)) = \tilde{x}_{cl}^{T}(\theta)X\tilde{x}_{cl}(\theta)$ for the closed-loop system such that $dV/d\theta < 0$. Thus, the state of the closed-loop system starting from $\tilde{x}_{cl}(\theta_0)$ will stay within an ellipsoid ε centered at the equilibrium point and defined by

$$\varepsilon = \left\{ \tilde{x}_{cl}(\theta) \middle| \tilde{x}_{cl}^{T}(\theta)X\tilde{x}_{cl}(\theta) \le \tilde{x}_{cl}^{T}(\theta_0)X\tilde{x}_{cl}(\theta_0) \right\}.$$

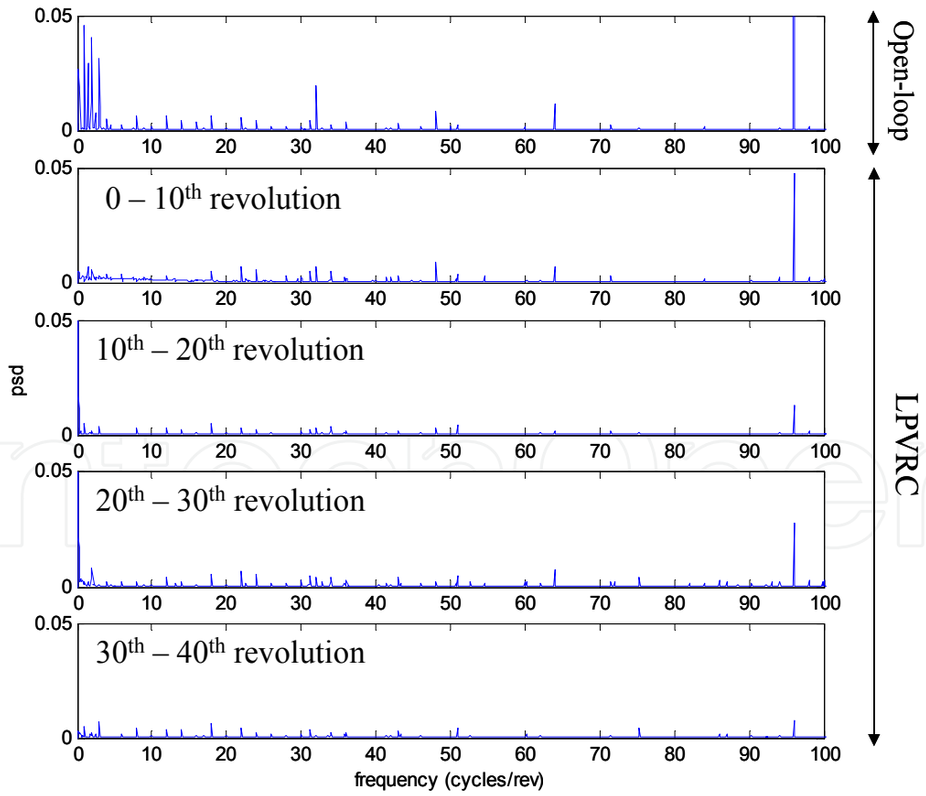

Fig. 14. Frequency spectra of the velocity signals for the open-loop and closed-loop systems. Spectra for the closed-loop system are divided into four, with each corresponding to signals measured from each 10-revolution interval (psd is abbreviation for power spectrum density)

The ellipsoid ε provides a bound for the state-dependent varying parameters, e.g., ρ. If a bound for the initial states can be established or estimated, a bound for the state-dependent varying parameters can be estimated, and the polytope Ψ which contains the parameter variation set $\bar{\Psi}$ can be determined more accurately. Since the proposed LPV control system has the property of being robust to unstructured but bounded uncertainty (specified by W_2 and Δ), the issues of measurement noise and uncertainty can be accounted for in the proposed formulation if they can be incorporated into the W_2 filter and the Δ block.

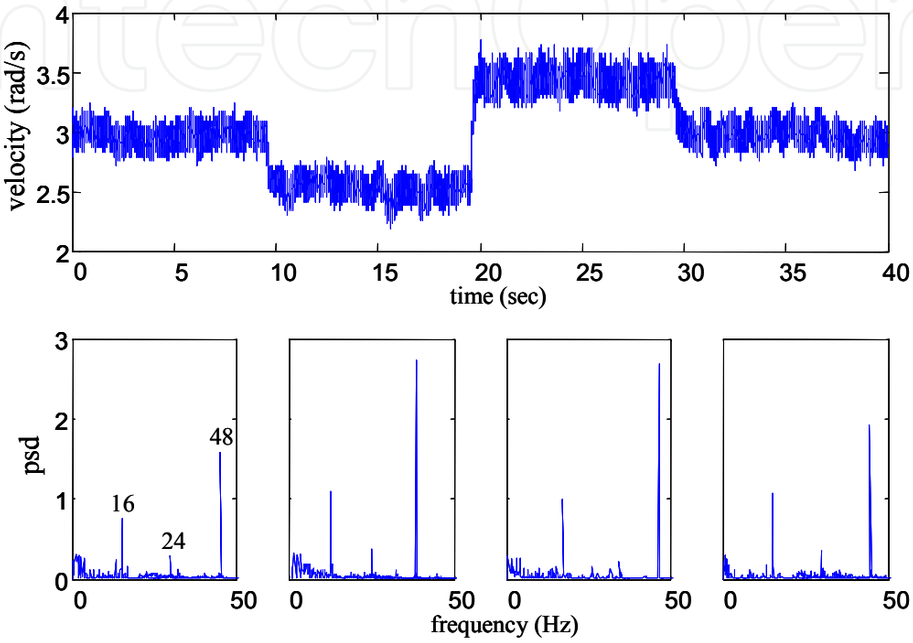

Fig. 15. Frequency spectra of the velocity signals for the closed-loop system using fixed period temporal repetitive control.

5. Conclusion

In this chapter, the notion of spatial-based repetitive control system and its historical development were introduced. Two designs, which were experimentally verified on a rotary motion system, representative of recent advancement in this field were presented. The designs, which are applicable to a generic class of LTI systems, address important practical issues such as actuator saturation and modelling uncertainty. However, several drawbacks and limitations are worth notice. First of all, the designs resorted to linear robust control paradigm and account for only unstructured uncertainty. It is well known that such control approach might lead to limited performance if information regarding the uncertainty (e.g., structure) is not properly utilized. Second, the LPVRC design relies on a common Lyapunov function, which also results in conservative design. The design is further degraded if the number of varying parameters increases or the varying parameter space is nonconvex. Finally, both designs along with other exiting ones are applicable only to rotary systems operating unidirectionally. The LPVRC design can improve by employing parameter varying Lyapunov function (Apkarian & Adams, 1998). On the other hand, since the open-loop spatial-based system, i.e., (3) or (6), is nonlinear, we may apply nonlinear control

paradigm to directly approach the nonlinearities. Existing nonlinear robust control schemes are capable of tackling various types of modelling uncertainty. Some have built-in parametric adaptation mechanism or can integrate with an existing parametric identification scheme to improve the performance of the design. Theoretical results (with numerical simulation) of several designs based on adaptive feedback linearization, adaptive backstepping, and adaptive iterative learning control have been reported (Chen & Yang, 2007, 2008, 2009; Yang & Chen, 2008, 2011).

6. References

Alter, D. M. & Tsao, T.-C. (1994). Two-dimensional exact model matching with application to repetitive control. *ASME Journal of Dynamic, Systems, Measurements and Control,* Vol. 116, pp. 2-9.

Apkarian, P., Gahinet, P., & Becker, G. (1995). Self-scheduled H^{∞} control of linear parameter varying systems: a design example. *Automatica,* Vol. 31, No. 9, pp. 1251-1261.

Apkarian, P., & Adams, R. J. (1998). Advanced gain-scheduling techniques for uncertain systems. *IEEE Transactions on Control Systems Technology*, Vol. 6, No. 1, pp. 21-32.

Becker, G., & Packard, A. K. (1994). Robust performance of linear parametrically varying systems using parametrically-dependent linear feedback. *Systems and Control Letters,* Vol. 23, No. 3, pp. 205-215.

Berkovitz, L. D. (2002). *Convexity and Optimization in* R^n , John Wiley & Sons, New York.

Chen, C.-L., & Chiu, G. T. C. (2001). Disturbance Rejection Using Two Degree of Freedom Repetitive Control Through Mixed Sensitivity Optimization. *Proceedings of 2001 ASME International Mechanical Engineering Congress and Exposition*, New York, NY.

Chen, C.-L., Chiu, G. T. C., & Allebach, J. P. (2003). Banding reduction in EP processes using human contrast sensitivity function shaped photoconductor velocity control. *J. Imaging Science and Technology,* Vol. 47, No. 3, pp. 209-223.

Chen, C.-L., Chiu, G. T. C.,& Allebach, J. P. (2006). Robust spatial-sampling controller design for banding reduction in electrophotographic process. *Journal of Imaging Science and Technology,* Vol. 50, No. 6, pp. 1-7.

Chen, C.-L., & Yang, Y.-H. (2007). Spatially periodic disturbance rejection for uncertain rotational motion systems using spatial domain adaptive backstepping repetitive control. *33rd Annual Conference of the IEEE Industrial Electronics Society*, Taipei, Taiwan, pp. 638-643.

Chen, C.-L., & Chiu, G. T. C. (2008). Spatially periodic disturbance rejection with spatially sampled robust repetitive control. *ASME Journal of Dynamic Systems, Measurement and Control,* Vol. 130, No. 2, pp. 11-21.

Chen, C.-L., & Yang, Y.-H. (2008). Spatial-based output feedback adaptive feedback linearization repetitive control of uncertain rotational motion systems subject to spatially periodic disturbances. *17th IFAC World Congress on Automatic Control*, Seoul, Korea, pp. 13151-13156.

Chen, C.-L., & Yang, Y.-H. (2009). Position-dependent disturbance rejection using spatial-based adaptive feedback linearization repetitive control. *International Journal of Robust and Nonlinear Control*, Vol. 19, pp. 1337-1363.

Chen, T., & Francis, B. (1995). *Optimal Sampled-Data Control Systems,* Springer, London, NY.

Cuiyan, L., & et al.. (2004). A survey of repetitive control. *Proceedings of IEEE International Conference on Intelligent Robots and Systems,* Sendai, Japan.

Francis, B. A., & Wonham, W. M. (1976). The internal model principle of control theory. *Automatica,* Vol. 12, No. 5, pp. 457-465.

Godler, I., Kobayashi, K., & Yamashita, T. (1995). Reduction of speed ripple due to transmission error of strain wave gearing by repetitive control. *International Journal of the Japan Society for Precision Engineering,* Vol. 29, No. 4, pp. 325-330.

Guo, L. (1997). Reducing the manufacturing costs associated with hard disk drives – A new disturbance rejection control scheme. *IEEE Transactions on Mechatronics,* Vol. 2, No. 2, pp. 77-85.

Gahinet, P., & Apkarian, P. (1994). A linear matrix inequality approach to H^{∞} control. *International Journal of Robust and Nonlinear Control,* Vol. 4, pp. 421-448.

Gahinet, P., & Apkarian, P. (1995). A convex characterization of gain-scheduled H^{∞} controllers. *IEEE Transactions on Automatic Control,* Vol. 40, No. 5, pp. 853-864.

Gahinet, P., Nemirovski, A., Laub, A. J., & Chilali. M. (1995). MATLAB LMI Control Toolbox, Mathworks.

Gahinet, P.,& et al. (1995). MATLAB LMI Control Toolbox, Mathworks, Natick, MA.

Gahinet, P. (1996). Explicit controller formulas for LMI-based H^{∞} synthesis. *Automatica,* Vol. 32, No. 7, pp.1007-1014

Garimella, S. S., & Srinivasan, K. (1996). Application of repetitive control to eccentricity compensation in rolling. *ASME Journal of Dynamic, Systems, Measurements and Control,* Vol. 118, pp. 657-664.

Hanson, R. D.,& Tsao, T. C. (2000). Periodic sampling interval repetitive control and its application to variable spindle speed noncircular turning process. *ASME Journal of Dynamic Systems, Measurements and Control,* Vol. 122, pp. 560-566.

Hara, S., Yamamoto, Y., Omata, T., & Nakano, M. (1988). Repetitive control system: A new type servo system for periodic exogenous signals. *IEEE Transactions on Automatic Control,* Vol. 33, No. 7, pp. 659-668.

Hillerstrom, G. (1996). Adaptive suppression of vibrations – A repetitive control approach. *IEEE Transactions on Control Systems Technology,* Vol. 4, No. 1, pp. 72-78.

Inoue,T., Nakano, M., & Iwai, S. (1981). High accuracy control of servomechanism for repeated contouring, *Proceeding of the 10th Annual Symposium on Incremental Motion Control Systems and Devices,* pp. 258-262.

Mahawan, B., & Luo, Z.-H. (2000). Repetitive control of tracking systems with time-varying periodic references. *International Journal of Control,* Vol. 73, No. 1, pp. 1-10.

Manayathara, T. J., Tsao, T. C., Bentsman, J., & Ross, D. (1996). Rejection of unknown periodic load disturbances in continuous steel casting process using learning repetitive control approach. *IEEE Transactions on Control Systems Technology,* Vol. 4, No. 3, pp. 259-265.

Moon, J. H., Lee, M. N., & Chung, M. J. (1998). Repetitive control for the track-following servo system of an optical disk drive. *IEEE Transactions on Control Systems Technology,* Vol. 6, No. 5, pp. 663-670.

Nakano, M., She, J. H., Mastuo, Y., & Hino, T. (1996). Elimination of position-dependent disturbances in constant-speed-rotation control systems. *Control Engineering Practice,* Vol. 4, pp. 1241-1248.

Onuki, Y., & Ishioka, H. (2001). Compensation for repeatable tracking errors in hard drives using discrete-time repetitive controllers. *IEEE/ASME Transactions on Mechatronics,* Vol. 6, No. 2, pp. 132-136

Rodriguez, H., Pons, J. L., & Ceres, R. (2000). A ZPET-repetitive speed controller for ultrasonic motors. *Proceeding of the 2000 IEEE International Conference on Robotics and Automation,* pp. 3654-3659.

Srinivasan, K., & Shaw, F. R. (1993). Discrete-time repetitive control system design using the regeneration spectrum. *ASME Journal of Dynamic Systems, Measurements and Control,* Vol. 115, No. 2A, pp. 228-237.

Tomizuka, M., Tsao, T. C., & Chew, K. K. (1989). Analysis and synthesis of discrete-time repetitive controllers. *ASME Journal of Dynamic Systems, Measurements and Control,* Vol. 111, No. 3, pp. 353-358.

Tung, E. D., Anwar, G., & Tomizuka, M. (1993). Low velocity friction compensation and feedforward solution based on repetitive control. *ASME Journal of Dynamic, Systems, Measurements and Control,* Vol. 115, pp. 279-284.

Wang, Y., & et al. (2009). Survey on iterative learning control, repetitive control, and run-to-run control. *Journal of Process Control,* Vol. 19, pp. 1589-1600.

Wit, C. C., & Praly, L. (2000). Adaptive eccentricity compensation. *IEEE Transactions on Control Systems Technology,* Vol. 8, No. 5, pp. 757-766.

Wu, F., Grigoriadis, K. M., & Packard, A. (2000). Anti-windup controller design using linear parameter-varying control methods. *International Journal of Control,* Vol. 73, No. 12, pp. 1104-1114.

Yamada, M., Riadh, Z., & Funahashi, Y. (1999). Design of discrete-time repetitive control system for pole placement and application. *IEEE Transactions on Mechatronics,* Vol. 4, No. 2, pp. 110-118.

Yang, Y.-H., & Chen, C.-L. (2008). Spatially periodic disturbance rejection using spatial-based output feedback adaptive backstepping repetitive control. *2008 American Control Conference*, Seattle, WA, pp. 4117-4122.

Yang, Y.-H., & Chen, C.-L. (2011). Spatial-based adaptive iterative learning control of nonlinear rotary systems with spatially periodic parametric variation. *International Journal of Innovative Computing, Information and Control*, Vol. x, pp. ????-????.

Zhou, K., & Doyle, J. (1997). *Essentials of Robust Control,* Prentice Hall.

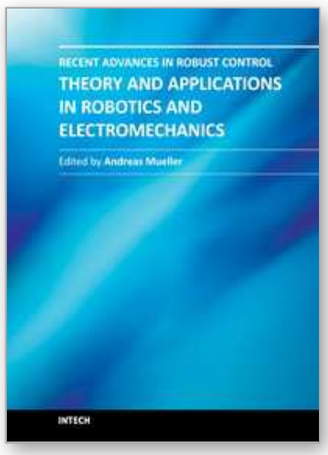

Recent Advances in Robust Control - Theory and Applications in Robotics and Electromechanics

Edited by Dr. Andreas Mueller

ISBN 978-953-307-421-4
Hard cover, 396 pages
Publisher InTech
Published online 21, November, 2011
Published in print edition November, 2011

Robust control has been a topic of active research in the last three decades culminating in H_2/H_\infty and \mu design methods followed by research on parametric robustness, initially motivated by Kharitonov's theorem, the extension to non-linear time delay systems, and other more recent methods. The two volumes of Recent Advances in Robust Control give a selective overview of recent theoretical developments and present selected application examples. The volumes comprise 39 contributions covering various theoretical aspects as well as different application areas. The first volume covers selected problems in the theory of robust control and its application to robotic and electromechanical systems. The second volume is dedicated to special topics in robust control and problem specific solutions. Recent Advances in Robust Control will be a valuable reference for those interested in the recent theoretical advances and for researchers working in the broad field of robotics and mechatronics.

How to reference

In order to correctly reference this scholarly work, feel free to copy and paste the following:

Cheng-Lun Chen and George T.-C. Chiu (2011). Spatially Sampled Robust Repetitive Control, Recent Advances in Robust Control - Theory and Applications in Robotics and Electromechanics, Dr. Andreas Mueller (Ed.), ISBN: 978-953-307-421-4, InTech, Available from: http://www.intechopen.com/books/recent-advances-in-robust-control-theory-and-applications-in-robotics-and-electromechanics/spatially-sampled-robust-repetitive-control

INTECH
open science | open minds

InTech Europe
University Campus STeP Ri
Slavka Krautzeka 83/A
51000 Rijeka, Croatia
Phone: +385 (51) 770 447
Fax: +385 (51) 686 166
www.intechopen.com

InTech China
Unit 405, Office Block, Hotel Equatorial Shanghai
No.65, Yan An Road (West), Shanghai, 200040, China
中国上海市延安西路65号上海国际贵都大饭店办公楼405单元
Phone: +86-21-62489820
Fax: +86-21-62489821

IntechOpen